Macromolecules

pubs.acs.org/Macromolecules

Article

Selective Protein Conjugation of Poly(glycerol monomethacrylate) and Poly(polyethylene glycol methacrylate) with Tunable Topology via Reductive Amination with Multifunctional ATRP Initiators for Activity Preservation

Filippo Moncalvo, Elisa Lacroce, Giulia Franzoni, Alessandra Altomare, Elisa Fasoli, Giancarlo Aldini, Alessandro Sacchetti, and Francesco Cellesi*

Cite This: *Macromolecules* 2022, 55, 7454–7468

Read Online

ACCESS | Metrics & More | Article Recommendations | Supporting Information

ABSTRACT: In this study, we compare poly(glycerol monomethacrylate) (PGMA) of different chain lengths and architectures (linear and two-arm) with poly(poly(ethylene glycol) methyl ether methacrylate) (PPEGMA) as an alternative polymer platform for the synthesis of a new generation of protein−polymer conjugates. Mono- and two-arm functional atom-transfer radical polymerization (ATRP) initiators were designed and selectively attached to lysozyme at the N-terminus via reductive amination. Site-specific, grafting from activator regenerated by electron transfer (ARGET) ATRP was carried out in phosphate buffer, and the reaction parameters were optimized to obtain polymer conjugates with predetermined molar mass and topology. The activity preservation under proteolytic and high-temperature conditions showed a clear dependence on the structure of the repeating unit and on the macromolecular architecture. These results highlighted the potential of PGMA as a poly(ethylene glycol) (PEG) alternative for the half-life extension of biotherapeutics. Moreover, this synthetic approach may inspire the design of a new class of protein−polymer conjugates through an optimal combination of macromolecular composition and topology.

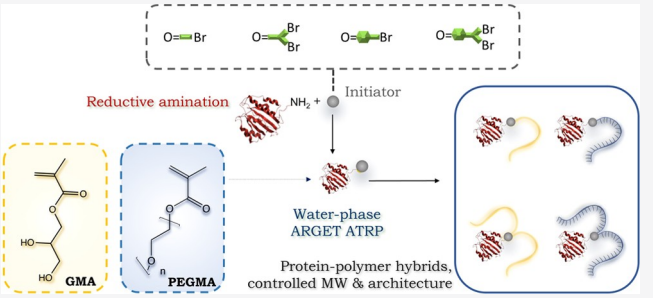

INTRODUCTION

Protein−polymer conjugates are currently employed in numerous applications in the field of bioengineering, biotechnology, and medicine.[1−4] Different strategies have been proposed in the past decades to graft polymers to active proteins (enzymes, therapeutic proteins), aiming to improve their stability in different environmental conditions.[4−6] Poly(ethylene glycol) (PEG) attachment (PEGylation) is presumably the best-known procedure, as several PEG−protein hybrids have been approved for clinical uses.[3,7,8] In fact, the covalent modification of therapeutic proteins with PEG provides steric shielding against immune activation and proteolytic degradation, while the increase in the molar mass reduces clearance by the kidneys, thus extending circulation half-life.[9,10] Although PEGylated proteins are widely used in clinics, significant limitations have recently emerged, which are mainly associated with PEG nondegradability,[11,12] antibody induction, and other immunogenic reactions.[13−15] Other synthetic polymers (including vinyl polymers,[16−18] polyglycerol,[7] polyoxazolines,[19] polyphosphoesters[20,21]) as well as natural and synthetic polysaccharides (such as polysialic acid,[22] trehalose glycopolymers,[23] alginate,[24] hyaluronic acid,[25] hydroxyethyl starch[26]) have been investigated as an alternative to PEG for half-life extension, exploring different syntheses and grafting methods.[3] Polymers are mainly conjugated using either a grafting-to or a grafting-from approach. In the grafting-to approach, a covalent bond is formed between reactive polymers and specific functional groups of a protein.[1,3,4,27] Different protein sites can be targeted, including the ϵ-amino groups of lysines, the N-terminal α-amino group of proteins, the thiol of cysteine residues, and the hydroxyl group of a serine or threonine.[3,4,27] This grafting-to strategy is typically characterized by low conversion due to the low concentration and the steric hindrance of the reactive groups, thus an additional purification step is required to remove the excess of the unreacted polymer.[28,29] Moreover, a random distribution of polymer chains grafted to multiple protein sites can be obtained if the conjugation conditions are not optimized, and this generally leads to a remarkable loss of activity.[4] The

Received: April 16, 2022
Revised: June 8, 2022
Published: June 27, 2022

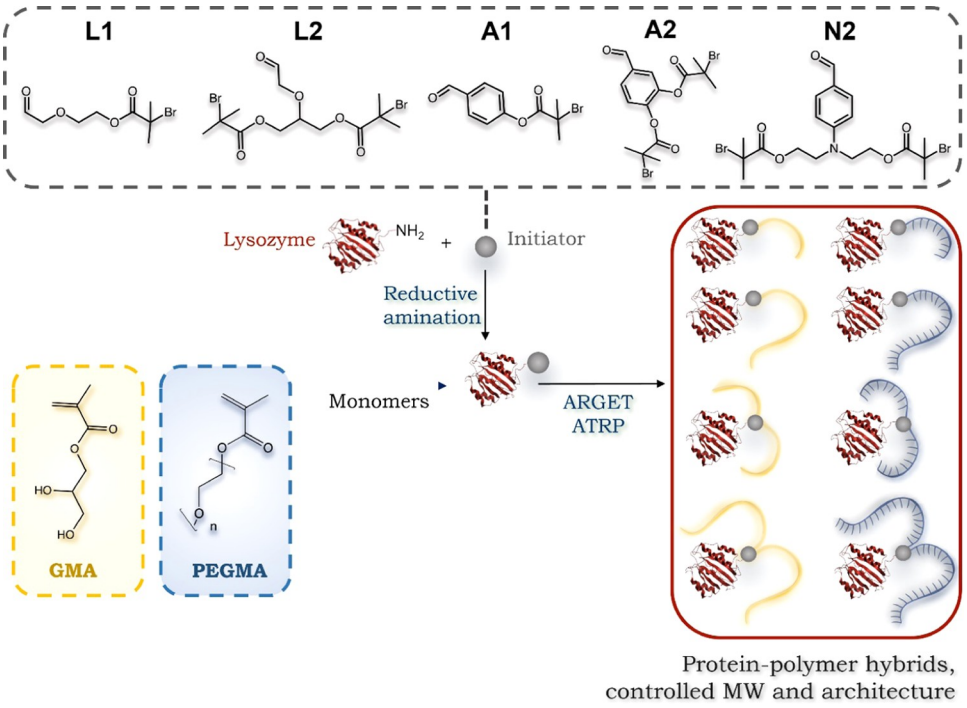

Figure 1. Synthesis and characterization of lysozyme−PGMA and lysozyme−PPEGMA conjugates.

grafting-from approach is based on polymerization, which initiates directly from a specific protein site.[30] A functional initiator is first attached to the protein via bioconjugation. A high yield of conjugation can be obtained due to the limited steric hindrance of this molecule,[31,32] and the final removal of the lower molar mass reagents is less challenging.[33,34] The main limitations are related to the control of polymerization under biorelevant conditions. Controlled-living polymerization techniques such as atom-transfer radical polymerization (ATRP), reversible addition−fragmentation chain-transfer polymerization (RAFT), and ring-opening metathesis polymerization (ROMP) have been recently investigated for site-specific polymer growth.[1,35−38] Aqueous-phase ATRP has been recently explored to obtain polymer−protein conjugates through the polymerization of poly(ethylene glycol) methyl ether methacrylate (PEGMA) macromonomers, grafted from recombinant hGH[31] and trypsin.[39] Activator regenerated by electron transfer (ARGET) ATRP in aqueous solutions has shown encouraging results for conjugation of therapeutic proteins,[40] achieving narrow molar mass distributions. Each grafting method presents advantages and limitations, thus no universal protein−polymer conjugation exists that could guarantee high stability while maintaining full activity for any class of proteins.[41]

A deeper understanding of the relation between the polymer physicochemical properties and ligand/biomolecule binding is needed to enhance the performance of these protein hybrids.[42−44] Therefore, the rational design of a protein−polymer conjugate for a specific application will be based on the appropriate selection of polymer type, its molar mass, and architecture, together with the selection of the optimized conjugation method and proper analytical characterization.

In this work, a new approach for protein−polymer conjugation was investigated to obtain site-specific grafting of hydrophilic biocompatible polymers with predetermined molar mass and topology.

To control the macromolecular architecture as well as the selectivity of the grafting site, different mono- and two-arm ATRP initiators functionalized with an aldehyde group were synthesized and attached to the proteins at the N-terminus via reductive amination to initiate polymerization at a protein site, which is not involved with the active domain (Figure 1). The reactions parameters were optimized by selecting lysozyme (LYS) as a model protein. ARGET ATRP was performed on these protein initiators in phosphate buffer to obtain macromolecules with stealth properties and high functionality. In terms of monomers and final polymer composition, glycerol monomethacrylate (GMA) was polymerized as well as PEGMA, and the effects of these two repeating units on protein activity and stability were investigated.

PGMA is a hydrophilic synthetic polymer, which has received high interest in biomedical research as alternative to PEG[45−51] since it presents low toxicity[47] and very limited interactions with proteins.[45,46,48] The two hydroxy groups per monomeric unit provide high hydrophilicity, minimize immune recognition, and can be easily functionalized to obtain different bioconjugated polymers.[50−52]

Different lysozyme−PPEGMA and lysozyme−PGMA conjugates were synthesized and characterized in terms of topology (linear, two-arm) and molar mass. Their enzymatic activity and stability in human serum and trypsin solution, as well as their thermal stability, were finally evaluated to identify optimal combinations of macromolecular composition and architecture for biopharmaceutical applications.

MATERIALS AND METHODS

Reagents and solvents, Amicon Ultra-15 Centrifugal Filters (cut off 3, 30 kDa), a lysozyme activity kit, a bicinchoninic acid (BCA) protein assay kit (Pierce), human serum (AB type), and trypsin from porcine pancreas (1000−2000 BAEE units/mg solid) were purchased from Sigma-Aldrich (Merck). *N*,*N*-Dimethylacetamide was purchased from Fisher Scientific and glycerol monomethacrylate was purchased from

https://doi.org/10.1021/acs.macromol.2c00783
Macromolecules 2022, 55, 7454−7468

Polysciences Europe. Deionized water was obtained from the Millipore Milli-Q purification unit.

Analytical Techniques. ^{1}H and ^{13}C NMR analyses were recorded on a Bruker Avance 400 MHz spectrometer at 298 K, using D_2O or $CDCl_3$ as solvents. Chemical shifts (δ) are reported in ppm downfield from the deuterated solvent as an internal standard, and coupling constants (J) are in Hz. Size exclusion chromatography (SEC) analyses were carried out with a JASCO instrument (2055 autosampler; RI-2031 refractive index detector; CO-2060 plus oven column; PU-2080 pump; three GRAM 300 mm × 8 mm (10 μm particle size) (1000, 100, 30 A) column; and a GRAM 50 mm × 8 mm (10 μm particle size) guard) using dimethylacetamide (DMAc) (30 mM LiBr) as an eluent at 1 mL/min at 40 °C. Samples were dissolved in DMAc at a concentration of 4 mg/mL. The average molar mass and dispersity were determined by standard calibration using linear PEG standards (M_n = 339 000, 197 000, 75 800, 30 700, 14 900, 6170, 1840, 560, 232 Da) (Sigma-Fluka).

Aqueous SEC was carried out on hydrolyzed polymers to determine their molar mass distributions. Dried polymers were dissolved in a 0.05 M Na_2SO_4 water/acetonitrile 80/20 v/v solution to obtain a concentration of 4 mg/mL and filtered through a 0.45 μm pore-size nylon membrane. The samples were analyzed using a Jasco 2000 system at a flow rate of 1 mL/min at 35 °C using 0.05 M Na_2SO_4 water/acetonitrile 80:20 v/v as an eluent, with a guard column and three Suprema columns (Polymer Standards Service; particle size 10 μm, pore sizes of 100, 1000, and 3000 Å). PEG standards (M_n = 232−339 000 Da, as reported above) were employed for the standard calibration.

Electrospray ionization mass spectrometry (ESI-MS) data for the characterization of the initiators were obtained using a Bruker Esquire 3000 PLUS (ESI Ion Trap LC/MS System), with an ESI source and a quadrupole ion trap detector (QIT) (needle 4.5 kV, N_2 flow rate 10 L/h, cone voltage 40 V) with a 13 000 (m/z) s^{-1} scan resolution over a mass range of m/z 35−500, by direct infusion of the methanol solution of analytes at 4 μL/min.

Synthesis of Aldehyde Functional Initiators. *2-(2-Oxoethoxy)ethyl 2-bromo-2-methylpropanoate (**L1**).* **L1** was synthesized according to a procedure described in previous work.[53] The steps of synthesis and the characterization of each precursor and the final product are reported in the Supporting Information.

*Synthesis of 2-(2-Oxoethoxy)propane-1,3-diyl bis(2-bromo-2-methylpropanoate) (**L2**). Step 1. Synthesis of 5-(2,2-Dimethoxyethoxy)-2-phenyl-1,3-dioxane.* 2-Phenyl-1,3-dioxan-5-ol (600 mg, 3.33 mmol, 1 equiv) was dissolved in 5 mL of *N*,*N*-dimethylformamide (DMF) and then NaH (60% dispersed in mineral oil) (266.4 mg, 6.66 mmol, 2 equiv) was added into microwave vial. The mixture was left under stirring for 20 min. Afterward, tetrabutylammonium bromide (53.67 mg, 0.1665 mmol, 0.05 equiv) dissolved in 1 mL of DMF was transferred into the reaction flask. Finally, bromoacetaldehyde diethyl acetal (751 μL, 4.99 mmol, 1.5 equiv) was dropped in and the reaction continued in the microwave (Biotage) for 2.5 h at 80 °C.

The mixture was then transferred in a separatory funnel and extracted with water. The aqueous solution was washed twice with diethyl ether. The organic phase was washed with brine and then dried with sodium sulfate. The purified product was dried under reduced pressure and further purified through a silica column using an eluent constituted by 70% hexane and 30% ethyl acetate. Yield: 70%

^{1}H NMR (400 MHz, $CDCl_3$) δ = 7.5 (dd, J = 7.7,1.19 Hz 2H, C$\underline{H}$−Ar), 7.33 (d, J = 7.3 Hz 3H,C$\underline{H}$−Ar), 5.5 (s, 1H, Ar−C$\underline{H}$(OCH_2)$_2$), 4.69 (t, J = 5.2 Hz, 1H, C$\underline{H}$(OCH_2CH_3)$_2$), 4.33 (m, 2H, OC$\underline{H_2}$CH), 4.02 (m, 2H, OC$\underline{H_2}$CH), 3.83−3.68 (m, 2H, CHC$\underline{H_2}$O), 3.67−3.52 (m, 4H, CH($OC\underline{H_2}CH_3$)$_2$), 3.42 (s, 1H), 1.23 (t, J = 5.3 Hz, 6H, CH($OCH_2C\underline{H_3}$)$_2$)

^{13}C NMR (100.59 MHz, $CDCl_3$, 298 K) δ = 138.3 (1C, Ar), 128.9 (1C, Ar), 128.3 (2C, Ar), 126.2 (2C, Ar), 102.2 (1C, $\underline{C}$H-(OCH_2CH_3)$_2$), 101.3 (1C, $(CH_2O)_2\underline{C}HC(CHCH)_2CH$), 71.4 (1C, $\underline{C}$H(CH_2O)$_2$), 70.0 (1C, CH$\underline{C}H_2O$), 69.2 (2C, CH($\underline{C}H_2O$)$_2$), 63.2 (2C, $CH_3\underline{C}H_2O$), 15.5 (2C, $\underline{C}H_3CH_2O$).

Step 2. Synthesis of 2-(2,2-Diethoxyethoxy)propane-1,3-diol. 5-(2,2-Dimethoxyethoxy)-2-phenyl-1,3-dioxane (230 mg, 0.7 mmol,1 equiv), 50 mL of tetrahydrofuran (THF), and palladium hydroxide on carbon (30 mg, 0.21 mmol, 0.3 equiv) were added in a two-neck flask. Three vacuum/hydrogen cycles were performed, and the mixture was left under a hydrogen atmosphere without stirring. The reaction continued under stirring for 4 h. Then, THF was removed under reduced pressure and the mixture was filtered through a Büchner funnel to remove palladium. The product was finally dried under reduced pressure. Yield: 78%.

^{1}H NMR (400 MHz, $CDCl_3$) δ = 4.58 (m, 1H, C$\underline{H}$(OCH_2CH_3)), 3.72−3.44 (m, 11H, ($OHC\underline{H_2}$)$_2$C$\underline{H}$O$C\underline{H_2}$, CH($OC\underline{H_2}CH_3$)$_2$), 1.21−1.10 (t, J = 5.3 Hz, 6H, CH($OCH_2C\underline{H_3}$)).

^{13}C NMR (100.59 MHz, $CDCl_3$, 298 K) δ = 101.3 (1C, $\underline{C}$H(OCH_2CH_3)$_2$), 81.8 (1C, $\underline{C}$H(CH_2OH)$_2$), 70.6 (1C, CH$\underline{C}H_2O$), 62.7 (2C, $CH_3\underline{C}H_2O$), 62.2 (2C, CH($\underline{C}H_2OH$)$_2$), 15.5 (2C, $\underline{C}H_3CH_2O$).

Step 3. Synthesis of 2-(2,2-Diethoxyethoxy)propane-1,3-diyl bis(2-bromo-2-methylpropanoate). 2-(2,2-Diethoxyethoxy)-propane-1,3-diol (300 mg, 1.56 mmol, 1 equiv) was weighed in a reaction flask. Then, 10 mL of THF and triethylamine (TEA) (652 μL, 4.68 mmol, 3 equiv) were added and the reactor was cooled in an ice bath. Then, α-bromoisobutyryl bromide (482 μL, 3.9 mmol, 2.5 equiv) was slowly dropped into the flask. After ice bath removal, the reaction continued overnight at room temperature. Afterward, THF was removed under reduced pressure and the mixture was transferred in a separatory funnel using ethyl acetate. The organic phase was extracted three times using a 1 M HCl solution to remove unreacted TEA and salts, and it was anhydrified with sodium sulfate. After filtration, the product was dried under reduced pressure and further purified with an automatic Biotage Selekt Systems with a silica column, using hexane for two elutions and then a gradient eluent until 80% hexane and 20% ethyl acetate. The purified product was finally dried under reduced pressure. Yield: 77%

^{1}H NMR (400 MHz, $CDCl_3$) δ = 4.62 (t, J = 5.1 Hz 1H C$\underline{H}$(OCH_2CH_3), 4.36−4.31 (m, 2H, C$\underline{H_2}$O), 4.30−4.26 (m, 2H, C$\underline{H_2}$O), 4.03−3.87 (m, 1H, C$\underline{H}CH_2O$), 3.77−3.66 (m, 4H, CH($OC\underline{H_2}CH_3$)$_2$)), 3.61−3.55 (m, 2H, OCH_2CH), 1.97 (s, 12H, ($C\underline{H_3}$)$_2$CBr), 1.23 (t, J = 5.3 Hz, 6H, CH($OCH_2C\underline{H_3}$)).

^{13}C NMR (100.59 MHz, $CDCl_3$) δ = 171.3 (2C, (O$\underline{C}$OC-(CH_3)$_2$Br)$_2$), 101.3 (1C, $\underline{C}$H (OCH_2CH_3)$_2$), 75.9 (1C, $\underline{C}$H-(CH_2O)$_2$), 71.6 (1C, CH$\underline{C}H_2O$), 64.6 (2C, (CH$\underline{C}H_2O$)$_2$), 62.7 (2C, $CH_3\underline{C}H_2O$), 55.6 (2C, ((CH_3)$_2\underline{C}$Br)$_2$), 30.7 (4C, (($\underline{C}H_3$)$_2$CBr)$_2$), 15.5 (2C, $\underline{C}H_3CH_2O$).

*Step 4. Synthesis of 2-(2-Oxoethoxy)propane-1,3-diyl bis(2-bromo-2-methylpropanoate) (**L2**).* A total of 60 mg of 2-(2,2-diethoxyethoxy)propane-1,3-diyl bis(2-bromo-2-methylpropanoate) (0.12 mmol) was dissolved in 2 mL of dichloromethane (DCM) and 2 mL of trifluoroacetic acid (TFA). The suspension was stirred at room temperature for 4 h and then 1 mL of Et_2O was added to remove TFA. The product was finally dried under reduced pressure. Yield: 96%

^{1}H NMR (400 MHz, $CDCl_3$) δ = 9.64 (s, 1H, $CH_2C\underline{H}O$), 4.35 (dd, J = 11.8, 4.4 Hz, 2H, C$\underline{H_2}$COH), 4.27−4.22 (m, 4H, CH(C$\underline{H_2}$O)$_2$), 3.91−3.84 (m, 1H, $CH_2C\underline{H}(CH_2)_2$), 1.88 (s, 12H, (($C\underline{H_3}$)$_2$CBr)$_2$).

^{13}C NMR (101 MHz, $CDCl_3$) δ = 199.7 (1C, $CH_2\underline{C}HO$), 171.3 (2C, (O$\underline{C}$OC(CH_3)$_2$Br)$_2$), 76.3 (1C, $\underline{C}H_2$COH), 75.9 (1C, $CH_2\underline{C}$H-(CH_2)$_2$), 64.3 (2C, (CH$\underline{C}H_2O$)$_2$), 55.3 (2C, ((CH_3)$_2\underline{C}$Br)$_2$), 30.7 (4C, (($\underline{C}H_3$)$_2$CBr)$_2$).

m/z: 487.1 [M + MeOH + K]$^+$, 1319.1 [3M + MeOH + K]$^+$.

*Synthesis of 4-Formylphenyl 2-bromo-2-methylpropanoate (**A1**).* 4-Hydroxybenzaldelhyde (1 g, 8.18 mmol, 1 equiv) was added to a two-neck flask and then 15 mL of THF was added, followed by triethylamine (TEA, 1.86 g, 18.4 mmol, 2.25 equiv). Then, the flask was cooled in an ice bath, and after 5 min, α-bromoisobutyrylbromide (2.82 g, 12.2 mmol, 1.5 equiv) was dissolved in 10 mL of THF with a dropping funnel. After the addition of 5 mL of THF to wash the funnel, the reaction continued overnight at room temperature. Afterward, THF was removed under reduced pressure, and the

https://doi.org/10.1021/acs.macromol.2c00783
Macromolecules 2022, 55, 7454−7468

sample was dissolved in ethyl acetate and extracted three times using a 1 M HCl solution to remove unreacted TEA and salts. The product was anhydrified with sodium sulfate, filtered, and dried under reduced pressure.

The product was further purified through a silica column using an eluent constituted of 80% hexane and 20% ethyl acetate. The product **A1** was finally collected and dried under reduced pressure. Yield: 86%.

^{1}H NMR (400 MHz, $CDCl_3$) δ = 10.01 (s, 1H, C$\underline{H}$O), 7.97−7.93 (m, 2H, Ar), 7.34−7.30 (m, 2H, Ar), 2.08 (s, 6H, $(C\underline{H_3})_2$CBr).

^{13}C NMR (101 MHz, $CDCl_3$) δ = 190.8 (1C, $\underline{C}$HO), 169.6 (1C, $\underline{C}$OOC), 155.4 (1C, Ar), 134.3 (1C, Ar), 131.3 (2C, Ar), 121.9 (2C, Ar), 54.9 (1C, $(CH_3)_2\underline{C}$Br), 30.7 (2C, $(\underline{C}H_3)_2$CBr).

m/z: 270.9 $[M + H]^+$, 294.9 $[M + Na]^+$, 324.9 $[M + MeOH + Na]^+$, 340.9 $[M + MeOH + K]^+$.

*Synthesis of 4-Formyl-1,2 phenylene bis(2-bromo-2-methylpropanoate) (**A2**).* 3,4-Dihydroxybenzaldelhyde (1 g, 7.24 mmol, 1 equiv) was added into a two-neck flask and then 20 mL of THF, followed by TEA (3.23 g, 32 mmol, 4.5 equiv). Then, the flask was cooled in an ice bath, and after 5 min, α-bromoisobutyryl bromide (4.98 g, 21.7 mmol, 3 equiv) dissolved in 10 mL of THF was added through a dropping funnel. Then, 3 mL of THF was also added to wash the funnel. The flask was removed from the ice and the reaction was continued overnight at room temperature. Afterward, THF was removed under reduced pressure, the sample was dissolved in ethyl acetate, and extracted three times using a 1 M HCl solution to remove unreacted TEA and salts. The product was anhydrified with sodium sulfate, filtered, and dried under reduced pressure. The product was further purified through a silica column using 90% hexane and 10% ethyl acetate as an eluent. The purified compound **A2** was collected and dried under reduced pressure. Yield: 90%.

^{1}H NMR (400 MHz, $CDCl_3$) δ = 10.00 (s, 1H, CC$\underline{H}$O), 7.84−7.79 (m, 2H, Ar), 7.45 (d, J = 8.1 Hz 1H, Ar), 2.07 (s, 12H, $((C\underline{H_3})_2CBr)_2$).

^{13}C NMR (101 MHz, $CDCl_3$) δ = 189.8 (1C, $\underline{C}$HO), 168.8 (1C, $\underline{C}$OOC$(CH_3)_2$Br), 168.5 (1C, $\underline{C}$OOC$(CH_3)_2$Br), 146.9 (1C, Ar), 142.8 (1C, Ar), 135.1 (1C, Ar), 128.5 (1C, Ar), 123.9 (1C, Ar), 123.8 (1C Ar), 54.6 (1C, $(CH_3)_2\underline{C}$Br), 54.6 (1C, $(CH_3)_2\underline{C}$Br), 30.7 (1C, $(\underline{C}H_3)_2$CBr), 30.6 (1C, $(\underline{C}H_3)_2$CBr).

m/z: 435.8 $[M + H]^+$, 450.9 $[M + Na]^+$, 474.8 $[M + K]^+$, 4.91 $[M + MeOH + Na]^+$.

*Synthesis of ((4-Formylphenyl)azanediyl)bis(ethane-2,1-diyl) bis(2-bromo-2-methylpropanoate) (**N2**).* 4-[*N*,*N*-Bis(2-hydroxyethyl)amino]benzaldehyde (400 mg, 1.912 mmol, 1 equiv) was dissolved with 9 mL of THF in a neck bottom flask and (580 mg, 5.7 mmol, 3 equiv) TEA was added. Then, the flask was cooled in an ice bath and 1.1 g of α-bromoisobutyryl bromide (4.78 mmol, 2.5 equiv) dissolved in 1 mL of THF was slowly dropped in. The flask was removed from ice and the reaction was continued overnight at room temperature.

Afterward, THF was removed under reduced pressure, the sample was dissolved in ethyl acetate, and extracted three times using a 1 M HCl solution to remove unreacted TEA and salts. The product was anhydrified with sodium sulfate, filtered, and dried under reduced pressure. The product was further purified through a silica column using 50% hexane and 50% ethyl acetate as an eluent. The purified compound **N2** was collected and dried under reduced pressure. Yield: 87%.

^{1}H NMR (400 MHz, $CDCl_3$) δ = 9.70 (s, 1H, C$\underline{H}$O), 7.71−7.67 (m, 2H, Ar), 6.80−6.76 (m, 2H, Ar), 4.33 (t, J = 6,0 Hz, 4H, $(NCH_2C\underline{H_2}O)_2$), 3.76 (t, J = 6,0 Hz 4H, $(NC\underline{H_2}CH_2O)_2$), 1.83 (s, 12H, $((C\underline{H_3})_2CBr)_2$).

^{13}C NMR (101 MHz, $CDCl_3$) δ = 190.2 (1C, C$\underline{H}$O), 171.6 (2C, $(CH_2\underline{C}OO)_2$), 151.9 (1C, Ar), 132.2 (1C, Ar), 126.5 (2C, Ar), 111.5 (2C, Ar), 62.7 (2C, $(NCH_2\underline{C}H_2O)_2$), 55.3 (2C, $((CH_3)_2\underline{C}Br)_2$), 49.1 (2C, $(NCH_2\underline{C}H_2O)_2$), 30.7 (4C, $((\underline{C}H_3)_2CBr)_2$).

m/z: 508.2 $[M + H]^+$, 530.2 $[M + Na]^+$, 1036.4 $[2M + Na]^+$.

Synthesis of PPEGMA. The polymerization of PEGMA generally followed this procedure ([M] = 0.33 mol/L, ascorbic acid feeding rate (FR_{AA}) = 8 nmol/min, phosphate-buffered saline (PBS) 100 mM, $CuBr_2$ = 9.8 × 10^{-5} mol/L): 50 mL of PBS 100 mM was added in a Schlenk tube, three cycles of vacuum/nitrogen were performed, and then nitrogen was flushed for 15 min. PEGMA (1.25 g, 2.5 mmol) was added in another Schlenk tube and three cycles of vacuum/nitrogen were carried out before adding 7.6 mL of purged PBS buffer. A total of 100 μL of an initiator (either 2-hydroxyethyl 2-bromoisobutyrate (HEBIB), **A1**, **A2**, **L1**, **L2**, or **N2**, 0.01 mmol for targeted degree of polymerization (DP) = 250 or 0.02 mmol for targeted DP = 125) from a stock solution in dimethyl sulfoxide (DMSO) (100 mM), 30 μL of $CuBr_2$ (0.17 mg, 0.76 μmol, 0.076 equiv), and tris(2-pyridylmethyl)amine (TPMA, 1.7 mg, 6 μmol, 0.6 equiv) from a stock solution ($CuBr_2$ 25 mM, TPMA 200 mM in buffer (PBS 100 mM)) were added to the Schlenk tube, which contained PEGMA, and the solution was purged for further 5 min. Next, 15 μL of an 8 mM ascorbic acid solution was added every 15 min to achieve an average rate of 8 nmol/min. The polymerization was performed at 25 °C. A total of 100 μL of the sample was collected from the reaction mixture at fixed time points for ^{1}H NMR and SEC analyses.

Synthesis of PGMA. The polymerization of GMA generally followed this procedure ([M] = 0.165 mol/L, FR_{AA} = 8 nmol/min, PBS 100 mM, $CuCl_2$ = 9.8 × 10^{-5} mol/L): 50 mL of PBS 100 mM was added in a Schlenk tube where, three vacuum/nitrogen cycles were carried out before flushing N_2 for 15 min. GMA (0.2 g, 1.25 mmol, 250 equiv) was added in another Schlenk tube and three vacuum/nitrogen cycles were carried out before adding 7.6 mL of purged PBS. A total of 50 μL of an initiator (either HEBiB, **A1**, **A2**, **L1**, **L2**, or **N2**, 0.005 mmol for targeted DP = 250 or 0.01 mmol for targeted DP = 125) from a DMSO stock solution (100 mM), 30 μL of $CuCl_2$ (0.1 mg, 0.76 μmol, 0.076 equiv), and TPMA (1.7 mg, 6 μmol, 0.6 equiv) from a $CuCl_2$/TPMA stock solution ($CuCl_2$ 25 mM, TPMA 200 mM in buffer (PBS 100 mM)) were added to the Schlenk tube, which contained GMA, and the solution was purged for 5 min. A total of 15 μL of an 8 mM ascorbic acid solution was added every 15 min to achieve an average rate of 8 nmol/min. The polymerization was performed at 25 °C. Then, 150 μL of the sample was collected from the reaction mixture at fixed time points for ^{1}H NMR and SEC analyses.

Procedure for Lysozyme-Initiator Conjugation. Hen egg-white (HEW) lysozyme (29.6 mg, 2.1 μmol,) and 2-methylpyridine borane (6.63 mg, 62 μmol) were added into a vial and dissolved in 10 mL of a solvent (PO_3^- 0.05M NaCl 0.1 M) adjusting the pH with 1 M HCl and 0.5 M NaOH to obtain the following pH values: 5.8, 6.1, 6.3, and 6.5. The aldehyde functional initiator (either **A1**, **A2**, **L1**, **L2**, or **N2**, 10.3 μmol) was added from a 500 mM stock solution in DMSO. The reaction proceeded at 35 °C under constant stirring. Then, 200 μL of the sample was collected at different time points (1−4 h) and stored at −20 °C before purification and high-performance liquid chromatography (HPLC)/ESI-MS analysis[53] (see the Supporting Information).

Polymerization from Lysozyme Initiators. *Conditions for PEGMA Polymerization.* A total of 12 mg of a lysozyme initiator (0.83 μmol, 1 equiv) dissolved in buffer at pH 6.3 (PO_3^- 0.05, NaCl 0.1 M) was purified using a 3 kDa cutoff Amicon filter and washed with 100 mM PBS. Afterward, the sample was concentrated to a final volume of 0.6 mL and transferred into a 3 mL Schlenk tube. Then, 103 mg of PEGMA (206 μmol, 250 equiv) was added, and three vacuum/nitrogen cycles were carried out under stirring. Then, 2.48 μL of a $CuBr_2$/TPMA solution ($CuBr_2$ 25 mM, TPMA 200 mM) was added to the mixture, which was cooled in a water−ice bath while degassing for 10 min. The reaction proceeded at a constant temperature (25 °C) while adding 1.25 μL of an ascorbic acid solution (1.41 mg/mL) every 15 min.

Conditions for PGMA Polymerization. A total of 6 mg of a lysozyme initiator (0.415 μmol, 1 equiv) dissolved in buffer at pH 6.3 (PO_3^- 0.05 M, NaCl 0.1 M) was purified using a 3 kDa cutoff Amicon filter and washed with 100 mM PBS. The sample was concentrated to a final volume of 0.6 mL and transferred into a small Schlenk tube. Then, 16.6 mg of GMA (103 μmol, 250 equiv) was added, and three vacuum/nitrogen cycles were carried out under stirring. A total of 2.48 μL of a $CuCl_2$/TPMA solution ($CuCl_2$ 25 mM, TPMA 200 mM)

https://doi.org/10.1021/acs.macromol.2c00783
Macromolecules 2022, 55, 7454−7468

Scheme 1. Synthetic Routes of the Functional Initiators

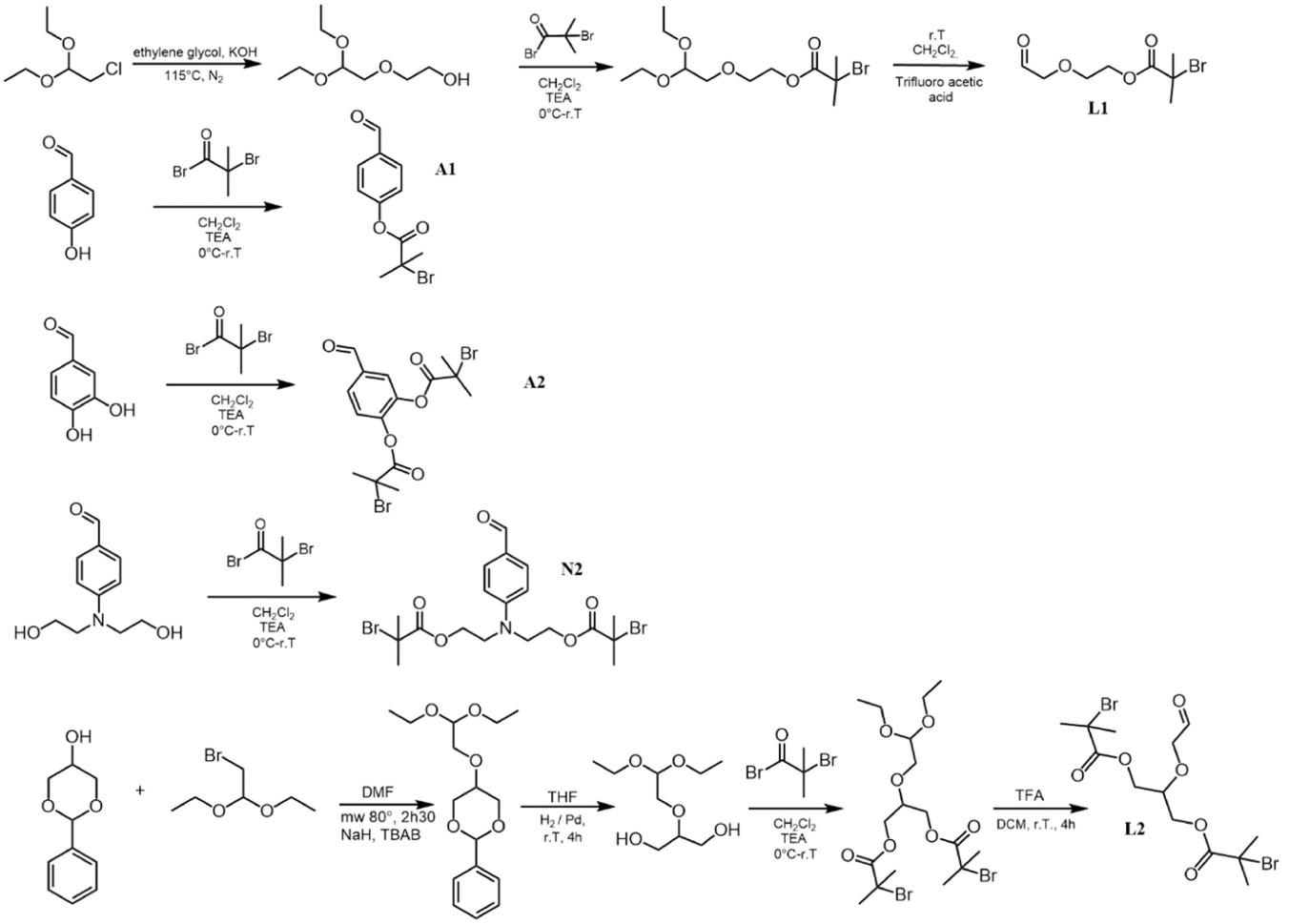

was added to the mixture, which was cooled in a water−ice bath and degassed for 10 min. The reaction proceeded at 25 °C while adding 1.25 μL of an ascorbic acid solution (1.41 mg/mL) every 15 min.

Purification and Analysis. A total of 100 μL of the final sample was purified by ultracentrifugation using an Amicon filter (30 kDa cutoff, 10 washing steps with 2 mL of deionized water to remove unreacted lysozyme, ATRP monomer, reagents, and salts). The waste was analyzed via ultraviolet−visible (UV−vis) spectroscopy (using a Jasco V-630 spectrophotometer, optical density measured at λ = 280 nm, using quartz cuvettes (Hellma QS) in a wavelength range of 200−2500 nm, optical path length 10 mm, 2.5 mL volume) to monitor the complete removal of unreacted lysozyme (Figure S14, Supporting Information), while the protein concentration achieved after purification was quantified by BCA assay.

Procedure for Kinetics Analysis. A total of 72.8 mg (0.005 mmol, 1 equiv) of protein initiator LYS−**L1** in solution was centrifuged, concentrated, and lyophilized directly into a Schlenk tube. Then, 3.8 mL of degassed 100 mM PBS and 619 μL of PEGMA (625 mg, 1.25 mmol, 250 equiv) were added and three vacuum/nitrogen cycles were carried out under stirring. A total of 15 μL of a $CuBr_2$/TPMA stock solution ($CuBr_2$ 25 mM, TPMA 200 mM) was added. Further, 7.5 μL of an ascorbic acid solution (1.41 mg/mL) was dropped every 15 min and the reaction was performed at 25 °C until reaching the desired conversion. Then, 50 μL of the sample was taken at fixed time points for NMR and SEC analyses. For comparison, polymerizations from the initiators **L1** and HEBIBB (0.005 mmol) were also carried out under the same experimental conditions.

Chain Extension. A total of 0.6 mL of 100 mM PBS containing 0.83 μmol (1 equiv) of PEGMA 100 **L1** (see Table 2 for details) was transferred into a 3 mL Schlenk tube. Then, 52 mg of PEGMA (03 μmol, 125 equiv) was added and three vacuum/nitrogen cycles were carried out under stirring. Next, 2.48 μL of a $CuBr_2$/TPMA solution ($CuBr_2$ 25 mM, TPMA 200 mM) was added to the Schlenk reactor. The ARGET ATRP was carried out according to the method reported above, and the final product was isolated and characterized according to the procedures used for the other lysozyme−polymer conjugates.

The hydrolysis of protein−polymer conjugates was obtained according to a procedure adapted from a previously published method[53] and is described in the Supporting Information.

Gel electrophoresis (sodium dodecyl sulfate−polyacrylamide gel electrophoresis (SDS−PAGE)) was performed as previously described[53] (Supporting Information).

The enzymatic activity of lysozyme−polymer conjugates in water, trypsin, and serum was evaluated using a lysozyme activity kit (Sigma-Aldrich) based on the *Micrococcus Lysodeikticus* test[53] (Supporting Information).

Thermal Stability. Lysozyme−protein conjugates or native lysozyme dissolved in ultrapure water at a concentration of 0.4 mg/mL were incubated at 90 °C for 30 min, 1, and 2 h. After cooling to room temperature, each solution was diluted to a concentration of 0.01 mg/mL, and the enzymatic activity was measured, according to the *M. Lysodeikticus* test. Data were presented as mean ± standard deviation of three different replicates and analyzed for statistical significance by unpaired two-tailed Student's *t*-test.

RESULTS AND DISCUSSION

Synthesis of Functional Initiators. A library of mono- and difunctional ATRP initiators containing an aliphatic or aromatic aldehyde was synthesized to evaluate their reactivity

https://doi.org/10.1021/acs.macromol.2c00783
Macromolecules 2022, 55, 7454−7468

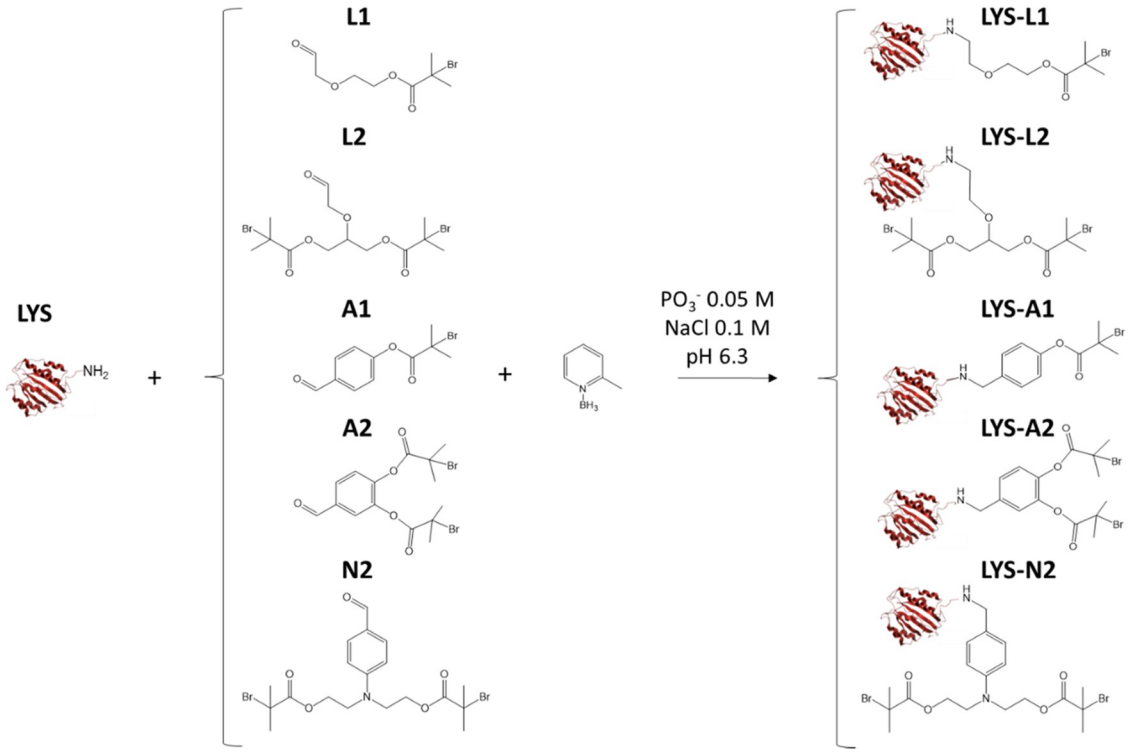

Figure 2. Structure of the initiators, their nomenclature, and conjugation with lysozyme.

and selectivity toward the protein N-terminus, as well as their capability to generate single or two-arm methacrylic polymers. Structures, nomenclature, and synthetic routes are reported in Scheme 1 and Figure 2. α-aldehyde monofunctional initiator **L1** was first selected and obtained as recently reported in the literature.[53,55] The difunctional initiator **L2** was synthesized by conjugating 2-phenyl-1,3-dioxan-5-ol with bromoacetaldehyde diethyl acetal to form 5-(2,2-dimethoxyethoxy)-2-phenyl-1,3-dioxane, followed by deprotection of the two hydroxyl groups and esterification with α-bromoisobutyryl bromide, and finally acetal deprotection to give the aldehyde. The monofunctional initiator **A1** was designed to obtain a benzaldehyde moiety while simplifying the synthetic procedure since this 4-formylphenyl 2-bromo-2-methylpropanoate was achieved by single-step esterification of 4-hydroxylbenzaldehyde with α-bromoisobutyryl bromide. Similarly, esterification of 3,4-dihydroxybenzaldehyde was carried out to synthesize the difunctional initiator **A2** (4-formyl-1,2 phenylene bis(2-bromo-2-methylpropanoate)). To obtain a benzaldehyde without the two sterically hindered 2-bromoisobutyrates in the ortho position, the difunctional initiator **N2** was also synthesized through esterification of 4-[*N*,*N*-bis(2-hydroxyethyl)amino]-benzaldehyde.

ARGET ATRP Optimization. Aqueous ARGET ATRP of PEGMA was first tested on each functional initiator, in the absence of protein, according to a protocol previously optimized.[40] The reaction was performed at 25 °C in 100 mM PBS with slow feeding (8 nmol/min) of ascorbic acid in the presence of a $CuBr_2$ catalyst (ratio Cu/monomer 300 ppm) with a tris(2-pyridylmethyl)amine (TPMA) ligand, PEGMA monomer concentration [M] = 0.33 M, and the functional initiator (**L1**, **L2**, **A1**, **A2**, **N2**) to obtain a maximum target degree of polymerization (DP) of 250. The control of the polymerization was confirmed by the semilogarithmic kinetic plot, which presented a linear trend after an induction period of ∼1 h, with no marked difference between the use of functional initiators and that of the commercial 2-hydroxyethyl 2-bromoisobutyrate (HEBIB) (Figure 3A). The polymers presented a relatively low dispersity (1.2−1.4) at conversions up to 90% (Figure 3B).

Under these reaction conditions, polymerization of GMA showed high levels of dispersity (1.5−1.7) (Figure S11, Supporting Information), which indicated a partial loss of control of the polymerization. ARGET ATRP of GMA was successfully improved by halving the molar concentration of the monomer and substituting the copper salt $CuBr_2$ with $CuCl_2$ since the lower reactivity of chloride led to higher control of the polymerization.[56] Under these conditions, the linear increase in the molar mass with conversion confirmed the first-order kinetics after an induction period of ∼2 h, which slightly varied depending on the type and functionality of the initiator tested (Figure 3C). The dispersity was found in the range of 1.25−1.35, maintaining a controlled character of up to ∼70% monomer conversion (Figure 3D). When the polymerizations were carried out at physiological PBS (10 mM), the dispersity increased (Figure S12, Supporting Information).

A summary of analytical results of the different polymerization conditions for different monomers and initiators is reported in Table 1. Reaction time and monomer conversion were optimized to obtain the highest DP while maintaining the dispersity of <1.4.

Initiator Conjugation. Each aldehyde functional initiator was conjugated with hen egg-white lysozyme at the N-terminus via reductive amination, with an imine linkage formed prior to reduction in situ to obtain a stable secondary amine.[3,57] N-terminal functionalization is a site-specific reaction that exploits the difference between the pK_a of the ϵ-amino group of lysine residues (9.3−10.5) and that of the N-terminal α-amino group of the proteins (7.6 to 8).[58] At optimal pH values (generally between 5.5 and 6.5), the N-terminus is

https://doi.org/10.1021/acs.macromol.2c00783
Macromolecules 2022, 55, 7454−7468

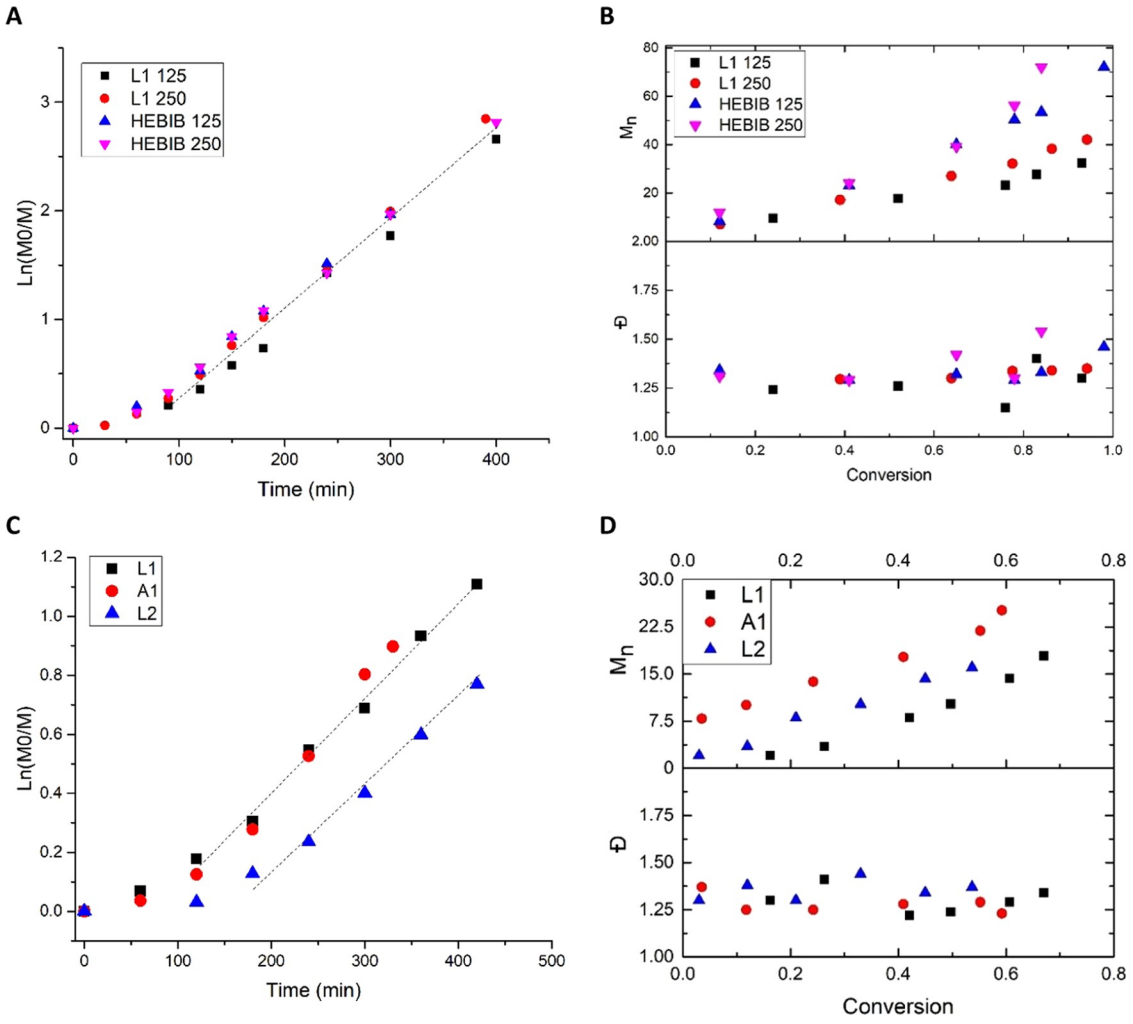

Figure 3. (A) Kinetic curves for aqueous ARGET ATRP of PEGMA (target DP 125 and 250, FR_{AA} = 8 nm/min) obtained from initiators L1 and HEBIB and (B) number average molar mass (M_n) and dispersity ($Đ$) vs conversion (PBS 100 mM; PEGMA 0.33 M; $[CuBr_2] = 9.8 \times 10^{-5}$ M). (C) Kinetic plot for GMA polymerization (target DP 125) from initiators **L1**, **A1**, and **L2** and (*D*) M_n and $Đ$ vs conversion (PBS 100 mM; GMA 0.165 M; $[CuCl_2] = 9.8 \times 10^{-5}$ M; FR_{AA} = 8 nm/min).

Table 1. Polymerization Conditions and Molar Mass Parameters of PPEGMA and PGMA Obtained from Different Initiators via ARGET ATRP in PBS 100 mM at T = 25 °C

initiator	M	DP	time (h)	conv (%)	$M_{n,NMR}$ (g/mol)	$M_{n,SEC}$ (g/mol)	$M_{w,SEC}$ (g/mol)	$Đ$
L1	GMA	125	7	67	13 666	17 900	24 000	1.34
L1	GMA	250	6	65	26 239	32 200	43 100	1.34
A1	GMA	125	6	59	12 133	25 100	31 000	1.23
L2	GMA	125	7	54	11 165	16 000	22 000	1.37
L1	PEGMA	125	7	93	58 383	32 400	42 200	1.30
L1	PEGMA	250	7	94	117 008	45 400	58 700	1.29
A1	PEGMA	125	4	83	52 146	21 100	26 000	1.23
A1	PEGMA	250	4	79	104 021	45 300	58 900	1.30
N2	PEGMA	125	4	73	46 132	22 800	31 300	1.37
A2	PEGMA	125	4	90	56 686	61 900	78 900	1.27
A2	PEGMA	250	4	99	124 186	214 400	277 500	1.29
L2	PEGMA	125	7	56	70 416	63 800	93 800	1.34
L2	PEGMA	250	7	45	56 666	96 800	128 700	1.33

unprotonated, while lysine residues are mainly protonated and unreactive.[59−61] Reductive amination at different pH values (5.8−6.5) and reaction times (up to 4 h) was therefore carried out to find the best condition for selective functionalization of the N-terminus, avoiding the formation of multiple initiation sites. An excess of 5 equiv of initiator per mol of protein was used, while the equivalents of the reducing agent 2-methylpyridine borane were also maintained constant. The samples were characterized by HPLC/ESI-MS (Figure 4A). The analysis showed evidence of the formation of a first

https://doi.org/10.1021/acs.macromol.2c00783
Macromolecules 2022, 55, 7454−7468

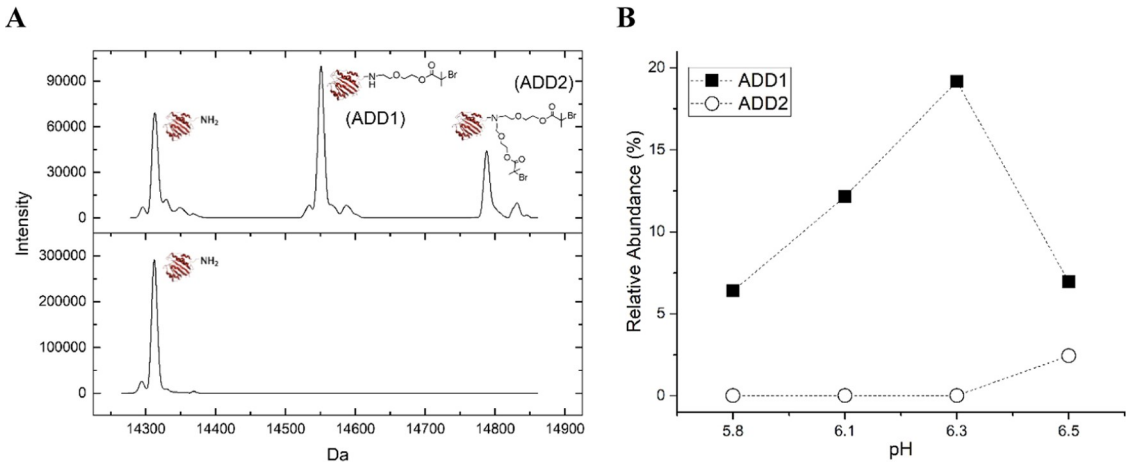

Figure 4. (A) HPLC/ESI-MS chromatograms of native LYS (below) and LYS−**L1** obtained by reductive amination (2 mg/mL protein solution, pH 6.3, 4 h). (B) Relative abundance (%) of adducts 1 and 2 (ADD1 and ADD2, respectively) obtained in 4 h at different pH values (5.8−6.5) (**L1**/LYS 5:1 mol/mol, LYS 1 mg/mL).

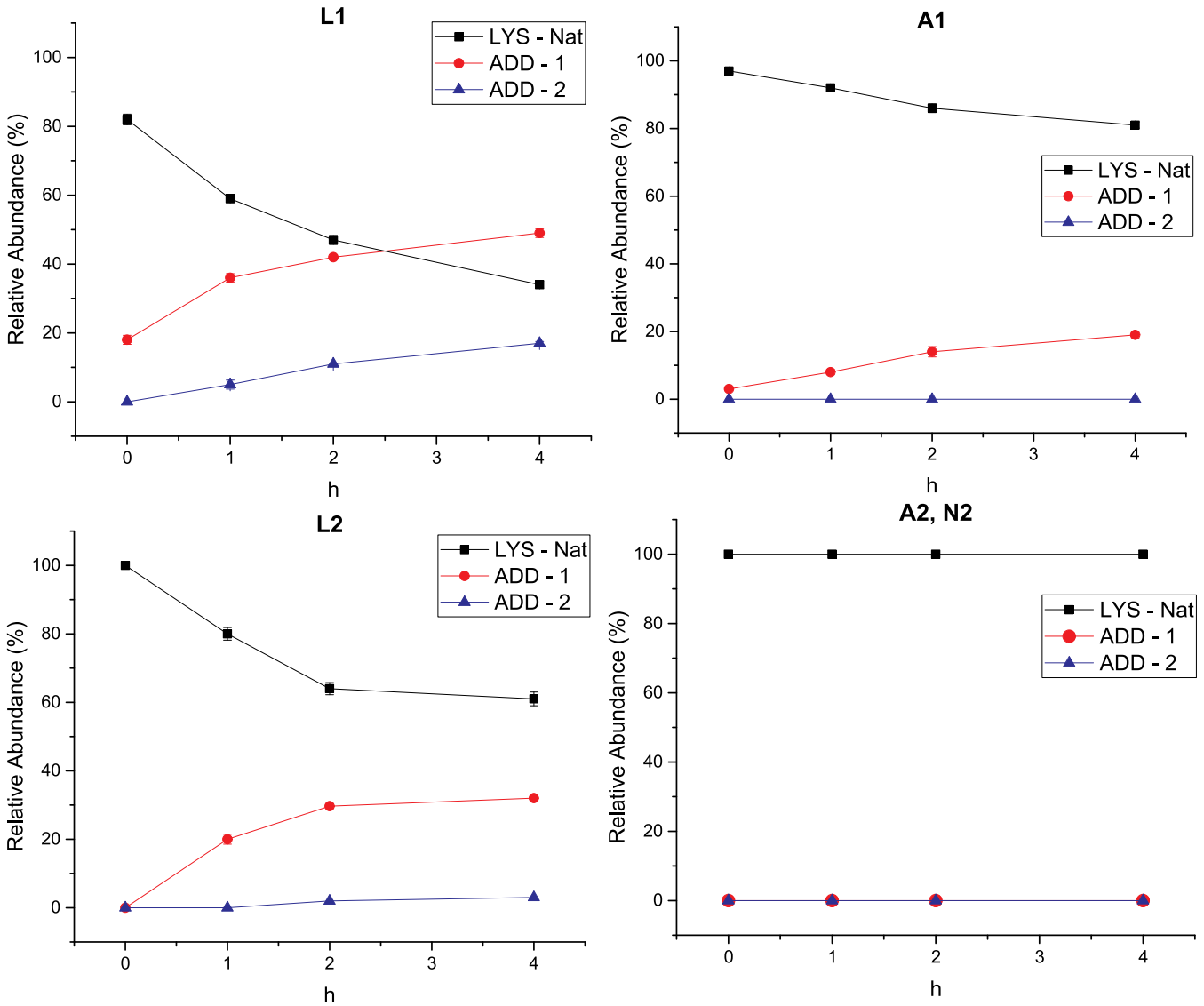

Figure 5. Kinetics of LYS conjugation with initiators **L1**, **A1**, **L2**, **A2**, and **N2** at pH 6.3. Relative abundance (%) of native LYS (LYS−Nat) and first and second adducts (ADD1, ADD2) measured at different time points (0−4 h) by HPLC/ESI-MS.

https://doi.org/10.1021/acs.macromol.2c00783
Macromolecules 2022, 55, 7454−7468

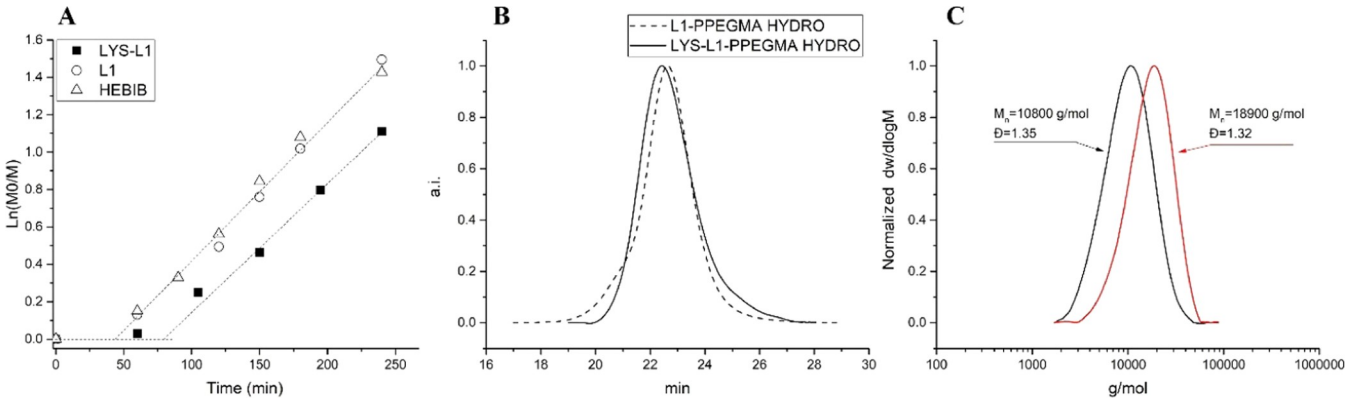

Figure 6. (A) Kinetic plot for aqueous ARGET ATRP of PEGMA (target DP 250) obtained from LYS−**L1** protein and the free initiators **L1** and HEBIB. (B) SEC chromatograph of the LYS−**L1**-PPEGMA conjugate and linear **L1**−PPEGMA (DP = 250) after hydrolysis. (C) SEC chromatograms of hydrolyzed **L1**−PPEGMA (DP = 125) before (black line) and after (red line) chain extension.

Table 2. Summary of the Polymers Synthesized from Lysozyme Initiators and Analyzed by ^{1}H NMR after Polymerization and by Aqueous SEC after Hydrolysis ($M_{n,NMR}$ Refers to the Hydrolyzed Polymer, and It Was Calculated as DP_{NMR}, M_{MMA}, where M_{MMA} is the Molar Mass of the Methacrylic Acid Monomeric Unit)[a]

name	I	M	M/I (mol/mol)	t (h)	χ (%)	DP_{NMR}	$M_{n,NMR}$ (g/mol)	$M_{n,SEC}$ (g/mol)	$M_{w,SEC}$ (g/mol)	$Đ$
GMA100A1	**A1**	GMA	125	2	83	104	8923	15 500	19 100	1.23
GMA200A1	**A1**	GMA	500	2	51	255	21 900	25 200	32 100	1.27
GMA100L1	**L1**	GMA	125	4	80	100	8600	15 000	18 900	1.25
GMA200L1	**L1**	GMA	250	4	70	175	15 050	21 700	31 900	1.47
GMA100L2	**L2**	GMA	125	5	74	93	3978 (x2)	8700	11 300	1.29
GMA200L2	**L2**	GMA	250	5	62	155	6650 (x2)	12 800	16 100	1.26
PEGMA100A1	**A1**	PEGMA	125	4	87	109	9353	13 300	17 400	1.31
PEGMA200A1	**A1**	PEGMA	250	4	80	200	17 200	18 400	22 900	1.24
PEGMA100L1	**L1**	PEGMA	125	2	95	119	10 212	11 000	15 300	1.38
PEGMA200L1	**L1**	PEGMA	250	2	90	225	19 350	22 400	27 000	1.20
PEGMA100L2	**L2**	PEGMA	250	7	50	125	5376 (x2)	6100	7400	1.22
PEGMA200L2	**L2**	PEGMA	250	7	100	250	10 750 (x2)	12 400	16 900	1.36

[a]For 2-arm polymers, $M_{n,SEC}$ refers to a single hydrolyzed arm.

adduct, which corresponds to the initiator grafted at the terminal NH_2, and a slower formation of a second adduct, which corresponds to bis-functionalization at the secondary amine.[61] Among different pH conditions (5.8−6.5), the most selective conjugation was obtained at pH 6.3 when a maximum conversion was achieved in the absence of bis-functionalization (Figure 4B).

At fixed pH (6.3), conjugation kinetics was monitored for all of the initiators synthesized, and mono- and bis-functionalized products were characterized in terms of conversion (Figure 5). **L1** showed good reactivity with the N-terminus since the LYS−**L1** conjugate reached a ∼49% conversion in 4 h. Unfortunately, also bis-functionalized species reached a non-negligible amount. To maintain a good selectivity, the reaction was stopped at 1 h to obtain a ∼36% conversion, while the relative abundance of bis-functionalized (4%) was sufficiently low. The **L2** initiator was also able to react efficiently, providing good selectivity and conversion since ∼33% of LYS−**L2** was formed in 4 h with a negligible amount of bis-functionalized species. **A1** was characterized by a lower aldehyde reactivity, as confirmed by a lower conversion (∼20% at 4 h). This result may be due to the steric hindrance of the aromatic ring as well as to the presence of oxygen as an electron-donating group. On the other hand, **A1** showed the advantage to avoid the formation of a bis-functionalized product under these conditions. **A2** and **N2** did not form any adduct during the reaction, suggesting that the presence of electron-donating groups (two oxygen atoms in the ortho position and nitrogen, respectively) did not favor the reactivity of benzaldehyde under these conditions. A further decrease in the pH value was not preferable, as it may favor protein denaturation.

The reaction parameters for each initiator were therefore fixed to maximize conversion of the first adduct while minimizing, if not avoiding, the formation of the second adduct (**L1**: 1 h, ADD1 36%, ADD2 4%, A1: 4h, ADD1 20%, ADD2 0%, L2: 4 h, ADD1 33%, ADD2 2%).

All protein conjugates were purified by centrifugal ultrafiltration before carrying out the grafting-from polymerization step.

Polymer Conjugation. The grafting polymerizations from lysozyme-conjugated initiators were carried out according to the optimized conditions for aqueous ARGET ATRP of PEGMA ad GMA. The polymerization of PEGMA from a relatively large amount of LYS−**L1** was tested to compare the reaction kinetics of this grafting-from polymerization with the corresponding ATRP in the absence of protein. The kinetic plot showed that in the first hour, the grafting-from polymerization was slightly slower than that obtained from the free aldehyde functional initiator (**L1**) and the commercial HEBIB (Figure 6A). This result may be due to the lower

https://doi.org/10.1021/acs.macromol.2c00783
Macromolecules 2022, 55, 7454−7468

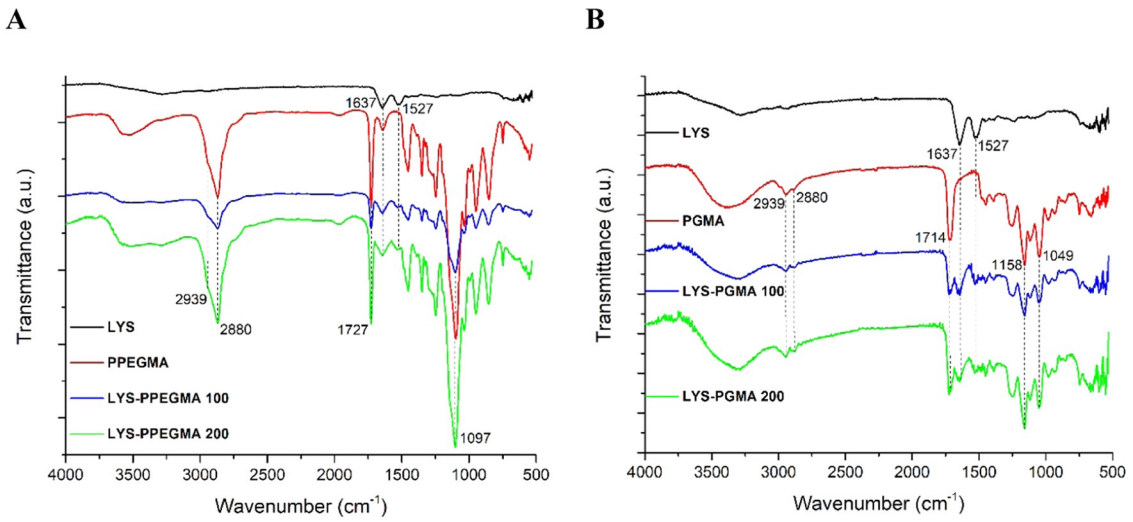

Figure 7. FTIR spectra of (A) LYS−PPEGMA conjugates and (B) LYS−PGMA conjugates (DP 100 and 200). Spectra of native lysozyme (LYS), and the polymers **L1**−PPEGMA and **L1**−PGMA (DP 100) are plotted for comparison.

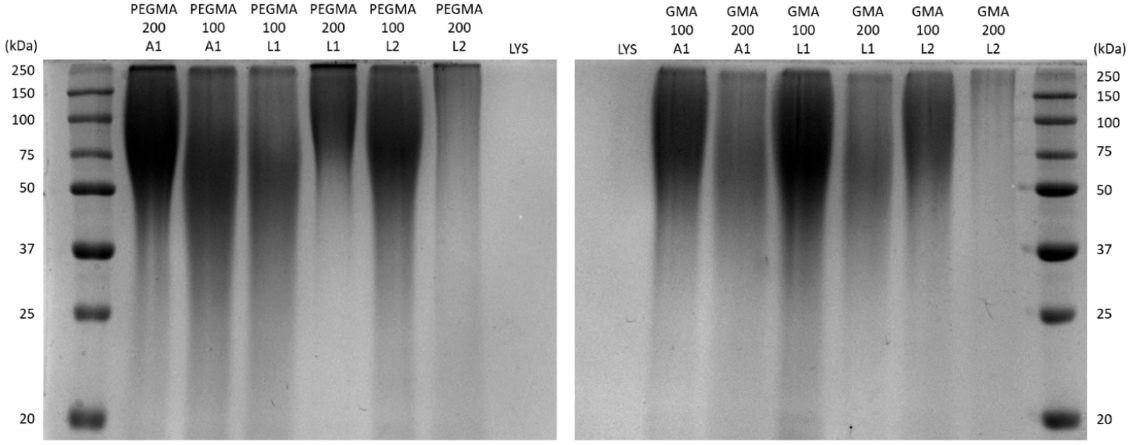

Figure 8. SDS−PAGE gel of lysozyme−polymer conjugates (LYS = native lysozyme).

reactivity of the LYS initiator as a consequence of the steric hindrance of the protein.

A method was also developed to achieve complete hydrolysis of the polymer and the protein (under strong basic or acid conditions) in each sample to isolate the methacrylate backbone (see the Supporting Information) for molar mass characterization. In fact, a direct SEC analysis of the protein−polymer hybrid is difficult since the protein is still folded in its active three-dimensional structure, and this would affect the correct determination of the molar mass of the polymer. The hydrolysis of the ester bonds led to a complete detachment of the polymer backbone from the lysozyme, as well as the cleavage of the side groups, thus poly(methacrylic acid) with the same degree of polymerization of the conjugated polymer was obtained (Figure S15, Supporting Information). The analysis confirmed that linear PPEGMA and LYS−PPEGMA synthesized at the same target degree of polymerization (DP = 250) showed an almost identical SEC chromatograph in water after hydrolysis (Figure 6B).

A library of lysozyme−polymer conjugates (based on PGMA and PPEGMA) at different targeted DP (100−200), 1-arm, and 2-arm was finally synthesized (Table 2). The products were purified and isolated by centrifugal ultrafiltration to remove the catalyst, unreacted species, and unbound enzymes (Figure S14, Supporting Information). To maintain the polymerizations under control in a relatively small volume, 20% excess monomer was generally used so that the target DP was obtained by stopping the reaction before reaching full conversion. For PGMA, we noticed an increase in the M_n by SEC data, as compared with NMR results. Anyway, the dispersity values were maintained relatively low (between 1.23 and 1.47). PEGMA chains provided better correspondence of the molar mass between NMR and SEC and lower dispersity too.

A chain extension test was also carried out to confirm the chain-end functionality and the living character of the polymerizations, as well as the absence of protein−polymer detachment by hydrolysis during the synthesis. Purified PEGMA100L1 was used as a macroinitiator for further PEGMA polymerization (target DP = 125). The reinitiation was complete, obtaining PPEGMA at an almost double molar mass, without increasing the dispersity, and with no evidence of dead chains in the SEC chromatogram (Figure 6C).

The successful polymer grafting was confirmed by the Fourier transform infrared spectroscopy (FTIR) spectrum of the purified products (Figure 7). LYS−PPEGMA conjugates showed the CH_2 and CH_3 stretching in the region 2990−2880 cm^{-1}, which are related to the PPEGMA chain (including the

https://doi.org/10.1021/acs.macromol.2c00783
Macromolecules 2022, 55, 7454−7468

O−C═O stretching characteristic of an ester group at 1727 cm^{-1} and C−O−C ester at 1097 cm^{-1}), as well as the amide I and amide II bands at 1637 and 1527 cm^{-1}, respectively, which are attributed to the α-helical and β-sheets of the lysozyme[62] (Figure 7A).

Similarly, LYS−PGMA conjugates presented the characteristic peaks of the PGMA chain, (the CH_2 and CH_3 stretching at 2990−2880 cm^{-1}, the C═O stretching at 1714, and that of C−O−C ester at 1158−1049 cm^{-1}),[45] as well as the amide I and amide II bands of lysozyme at 1637 and 1527 cm^{-1} (Figure 7B).

Gel electrophoresis (SDS−PAGE) was carried out to further document the effect of the grafted polymers on the electrophoretic mobility of protein−polymer hybrids.[23,31,63] Conjugate formation was evident by the shift to the high molar mass of the lysozyme covalently bound to PPEGMA and PGMA (Figure 8), whereas the native lysozyme (~14 kDa) was not retained in these 12% acrylamide gels. It was known that the method was unable to provide a clear separation of the polymer-grafted proteins in terms of the molar mass. In fact, broad or smeared bands of PEGylated proteins are generally obtained due to the complex interaction between PEG chains and SDS micelles and PEG chains and proteins.[64−66] In our case, PGMA also showed the same behavior, suggesting a similar interaction with the gel as with PEG.

Activity of Protein−Polymer Conjugates. The enzymatic activity of the protein−polymer conjugates was determined against substrate *M. Lysodeikticus*.[18,54,67] Remarkably, lysozyme−PEGMA and lysozyme−PGMA still provided intense enzymatic activity, which was between 70 and 90% of the corresponding activity of the untreated naked lysozyme tested under the same conditions (Figure 9). These results showed that the PEGMA and PGMA conjugation did not cause substantial alterations in protein stability and accessibility of the active binding site. No significant difference in activity was noticed between conjugates synthesized from the **A1** and **L1** initiators, respectively. At fixed DP, higher activity was noticed for PGMA than for PPEGMA, which can be easily explained by the lower molar mass of GMA repeating units than that of PEGMA. As expected, by fixing the polymer type (either PGMA or PPEGMA), a slight decrease in activity was obtained when the DP increased, although this difference was not always statistically significant.

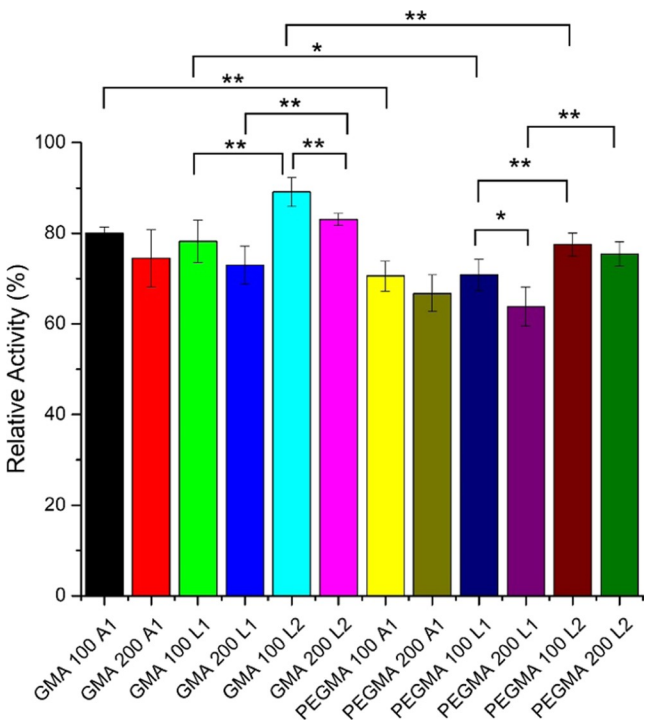

Figure 9. Enzymatic activity of different LYS−PPEGMA and LYS−PGMA conjugates (100% relative activity refers to native lysozyme) (N = 3, *P < 0.1, **P < 0.05).

At fixed DP (either 100 or 200), the two-arm polymers presented higher activity for both PPEGMA and PGMA, thus indicating that macromolecular architecture may play a crucial role in preserving the enzymatic activity. In fact, it may be hypothesized that the two-arm topology presents a denser and more compact macromolecular domain than a linear polymer chain,[42] thus providing less steric hindrance to the active domain of the protein.[68,69]

Comparing polymers with the same DP per arm (**L1** 100 vs **L2** 200 for both PGMA and PPEGMA), the difference in activity was not statistically significant. This result may be ascribed to the opposite effects of lowering activity with larger M_n while enhancing it with the two-arm architecture. In summary, PGMA 100 **L2** was the polymer that provided the highest lysozyme activity (~90%).

The stability against enzymatic degradation was evaluated by testing the lysozyme activity following incubation in human serum and a trypsin solution for 4 h (Figure 10). In fact, the incubation in serum represents a valuable test to assess protein stability against hydrolytic enzymes of the blood,[62,70,71] while trypsin is a serine protease that is known to hydrolyze proteins at the carboxyl side of lysine or arginine.[62,72] Remarkably, while the activity of native lysozyme decreased by ~40% both in serum and in trypsin, polymers guaranteed higher protection from protease degradation. In terms of retained activity (i.e., the ratio between activity after incubation and activity before incubation), the conjugates functionalized with PPEGMA were characterized by higher performance, reaching a retained activity of up to 96%, suggesting that the large PEG side chain provided more stability than the diol unit in GMA.

Regarding the stability in serum, no clear difference in retained activity was appreciated between **A1** and **L1** initiators (Figure 10A). Unexpectedly, a negligible difference was appreciated for different DP of the same polymer type (PGMA or PPEGMA). On the other hand, at fixed DP (either 100 or 200), the two-arm polymers presented higher retained activity for both PGMA and PPEGMA, thus indicating that macromolecular architecture may also contribute to the protection of proteins against enzymatic hydrolysis. These data are consistent with a greater surface area of protein covered by branched polymers,[68] and the denser macromolecular domain of the two-arm topology may limit the interactions between the protein−polymer hybrid and the hydrolytic enzymes.[42] According to these results, the two-arm polymers seem to maximize both activity and stability.[68,69] Comparing polymers with the same DP per arm (**L1** 100 vs **L2** 200, both for PGMA and PPEGMA), the stability increased with the number of arms, particularly for PGMA. This result further confirmed the positive effect of two-arm versus one-arm topology. The differences were not statistically significant for PPEGMA, although we noticed that the retained activity was already >80% for all PPEGMA conjugates, and this could affect data interpretation.

https://doi.org/10.1021/acs.macromol.2c00783
Macromolecules 2022, 55, 7454−7468

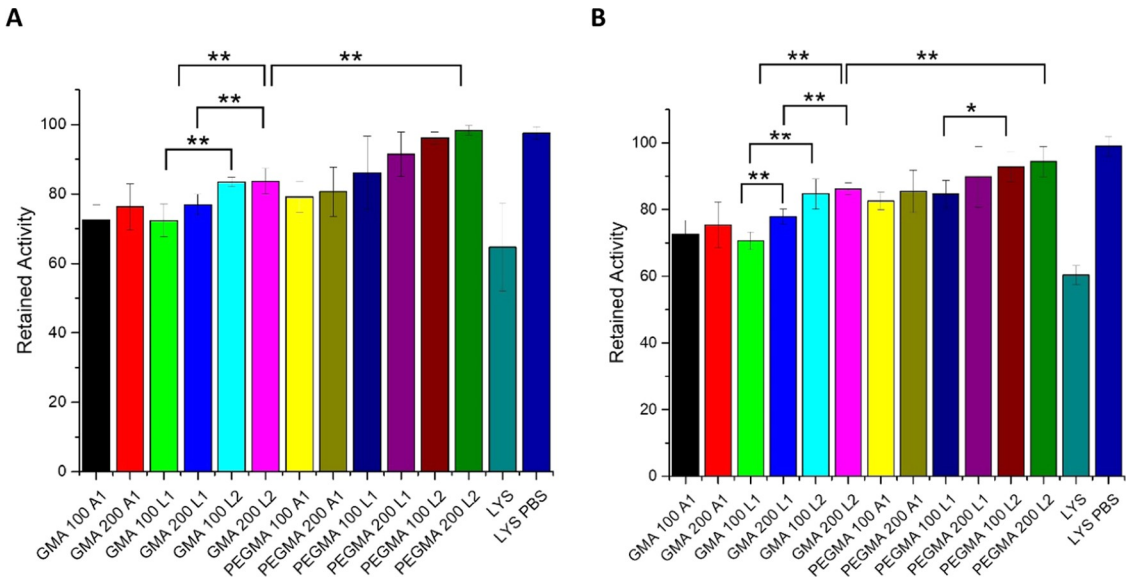

Figure 10. Retained activity of different LYS−PPEGMA and LYS−PGMA incubated for 4 h in serum (A) and trypsin (B) (LYS PBS = native lysozyme incubated in PBS 10 mM, pH 7.4) (N = 3, *P < 0.1, **P < 0.05).

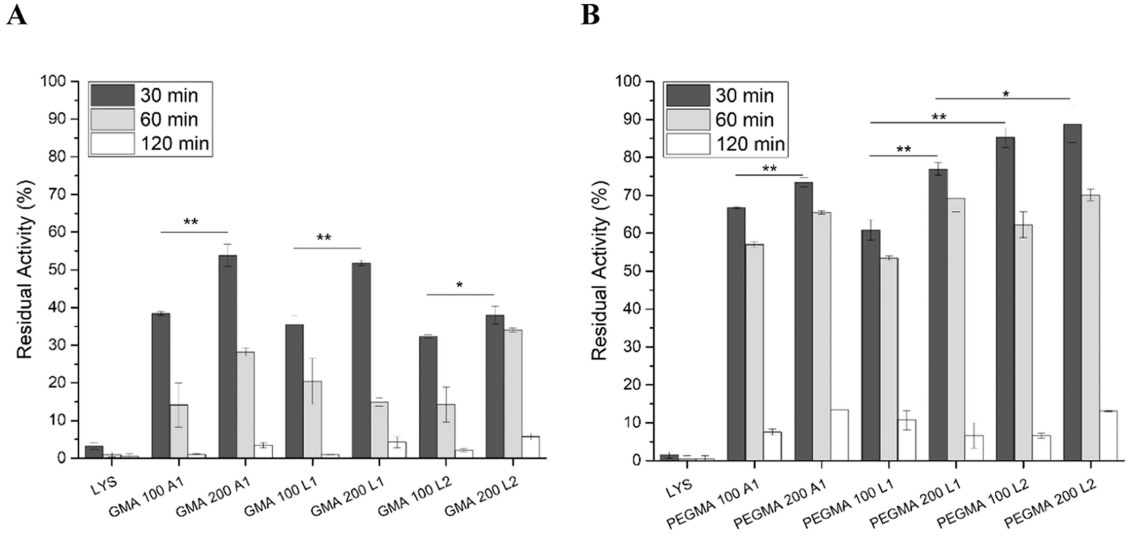

Figure 11. Residual activity of LYS−PGMA (A) and LYS−PPEGMA conjugates (B) after incubation at 90 °C for 30, 60, and 120 min (LYS = native lysozyme) (N = 3, *P < 0.1, **P < 0.05).

Treatment with trypsin showed similar results as with serum (Figure 10B). In this case, a difference in retained activity between GMA 100 **L1** and 200 **L1** was noticed, which indicated a positive effect of a larger molar mass on stability. The different activity values between PEGMA 200 **L1** and PEGMA 200 **L2** further confirm the protective effect of the two arms under these conditions.

Finally, the thermal stability of the conjugates was evaluated after incubation in an aqueous solution at 90 °C under conditions that induce the denaturation of both tertiary and secondary structures of lysozyme at T_m values in the range of 74−75 °C.[73] Native lysozyme was almost completely denatured in 30 min, while all polymer conjugates maintained a residual activity even after 60 min, before a major loss at 2 h (Figure 11). At 30 min, GMA 200 **L1** and GMA 200 **A1** showed the highest residual activity (52−54%) among PGMA conjugates, which confirmed the higher stabilizing effect of polymers with a larger molar mass. The two-arm topology of PGMA did not show any substantial improvement over the single arm; GMA 200 **L2** presented only a ∼38% residual activity at 30 min, although this value did not decrease substantially after 60 min (Figure 11A). PPEGMA provided the highest thermal stability, with PEGMA 200 **L2** showing almost 90% of residual activity after 30 min and 70% after 1 h (Figure 11B).

This enhanced stabilizing effect may be due to the larger PEG side chains than the GMA units, as well as to the possible partial dehydration of PPEGMA at high temperatures (PPEGMA is known to have a lower critical solution temperature (LCST) transition at 85−90 °C[74,75]), which may further protect lysozyme from denaturation.[76] The higher stabilizing effect of larger molar mass PPEGMA was also confirmed, and the best performance was obtained with PEGMA 100 **L2** and PEGMA 200 **L2**, suggesting a protective effect of the two-arm architecture in this case as well.

https://doi.org/10.1021/acs.macromol.2c00783
Macromolecules 2022, 55, 7454−7468

CONCLUSIONS

Mono- and difunctional ATRP initiators containing an aliphatic or aromatic aldehyde were successfully synthesized, and their grafting to lysozyme at the N-terminus was evaluated. Aqueous ARGET ATRP parameters were optimized for the polymerization of PEGMA and GMA. Lysozyme−PPEGMA and lysozyme−PGMA with different numbers of arms and molar masses were isolated and characterized. Their enzymatic activity after polymerization was preserved and showed a dependence on the chemistry of the repeating unit and on the molar mass of the polymer chains. An effect of macromolecular architecture was also highlighted, with the two-arm topology which presented higher activity than its one-arm counterpart. Similar results were obtained with stability tests on serum and trypsin, and at high temperature, which confirmed that a proper design of polymer architecture may help reduce enzymatic degradation.

ASSOCIATED CONTENT

Supporting Information

The Supporting Information is available free of charge at https://pubs.acs.org/doi/10.1021/acs.macromol.2c00783.

Experimental protocols, ^{1}H NMR, ^{13}C NMR of initiators and their precursors, kinetic plots for aqueous ARGET ATRP, macromolecule purification and hydrolysis, and ^{1}H NMR and SEC of polymers (PDF)

AUTHOR INFORMATION

Corresponding Author

Francesco Cellesi − *Department of Chemistry, Materials and Chemical Engineering "G. Natta", Politecnico di Milano, Milano 20131, Italy;* orcid.org/0000-0001-6106-9317; Phone: +39-02-23993099; Email: francesco.cellesi@polimi.it

Authors

Filippo Moncalvo − *Department of Chemistry, Materials and Chemical Engineering "G. Natta", Politecnico di Milano, Milano 20131, Italy*

Elisa Lacroce − *Department of Chemistry, Materials and Chemical Engineering "G. Natta", Politecnico di Milano, Milano 20131, Italy*

Giulia Franzoni − *Department of Chemistry, Materials and Chemical Engineering "G. Natta", Politecnico di Milano, Milano 20131, Italy*

Alessandra Altomare − *Department of Pharmaceutical Sciences (DISFARM), University of Milan, 20133 Milan, Italy*

Elisa Fasoli − *Department of Chemistry, Materials and Chemical Engineering "G. Natta", Politecnico di Milano, Milano 20131, Italy;* orcid.org/0000-0002-7370-993X

Giancarlo Aldini − *Department of Pharmaceutical Sciences (DISFARM), University of Milan, 20133 Milan, Italy*

Alessandro Sacchetti − *Department of Chemistry, Materials and Chemical Engineering "G. Natta", Politecnico di Milano, Milano 20131, Italy;* orcid.org/0000-0002-4830-0825

Complete contact information is available at: https://pubs.acs.org/10.1021/acs.macromol.2c00783

Notes

The authors declare no competing financial interest.

ACKNOWLEDGMENTS

This research project was funded by Regione Lombardia (POR FESR 2014−2020) within the framework of the NeOn project (ID 239047) and the NEWMED project (ID 1175999).

REFERENCES

(1) Cohen-Karni, D.; Kovaliov, M.; Ramelot, T.; Konkolewicz, D.; Graner, S.; Averick, S. Grafting challenging monomers from proteins using aqueous ICAR ATRP under bio-relevant conditions. *Polym. Chem.* **2017**, *8*, 3992−3998.

(2) Bontempo, D.; Maynard, H. D. Streptavidin as a Macroinitiator for Polymerization: In Situ Protein−Polymer Conjugate Formation. *J. Am. Chem. Soc.* **2005**, *127*, 6508−6509.

(3) Moncalvo, F.; Martinez Espinoza, M. I.; Cellesi, F. Nanosized delivery systems for therapeutic proteins: clinically validated technologies and advanced development strategies. *Front. Bioeng. Biotechnol.* **2020**, *8*, No. 89.

(4) Wang, Y.; Wu, C. Site-Specific Conjugation of Polymers to Proteins. *Biomacromolecules* **2018**, *19*, 1804−1825.

(5) Pelegri-O'Day, E. M.; Lin, E. W.; Maynard, H. D. Therapeutic Protein-Polymer Conjugates: Advancing Beyond PEGylation. *J. Am. Chem. Soc.* **2014**, *136*, 14323−14332.

(6) Boyer, C.; Bulmus, V.; Liu, J.; Davis, T. P.; Stenzel, M. H.; Barner-Kowollik, C. Well-Defined Protein−Polymer Conjugates via in Situ RAFT Polymerization. *J. Am. Chem. Soc.* **2007**, *129*, 7145−7154.

(7) Tully, M.; Dimde, M.; Weise, C.; Pouyan, P.; Licha, K.; Schirner, M.; Haag, R. Polyglycerol for Half-Life Extension of Proteins—Alternative to PEGylation? *Biomacromolecules* **2021**, *22*, 1406−1416.

(8) Walsh, G. Biopharmaceutical benchmarks 2018. *Nat. Biotechnol.* **2018**, *36*, 1136−1145.

(9) Grigoletto, A.; Maso, K.; Mero, A.; Rosato, A.; Schiavon, O.; Pasut, G. Drug and protein delivery by polymer conjugation. *J. Drug Delivery Sci. Technol.* **2016**, *32*, 132−141.

(10) Owens, D. E., III; Peppas, N. A. Opsonization, biodistribution, and pharmacokinetics of polymeric nanoparticles. *Int. J. Pharm.* **2006**, *307*, 93−102.

(11) Ivens, I. A.; Achanzar, W.; Baumann, A.; Braendli-Baiocco, A.; Cavagnaro, J.; Dempster, M.; Depelchin, B. O.; Rovira, A. R. I.; Dill-Morton, L.; Lane, J. H.; Reipert, B. M.; Salcedo, T.; Schweighardt, B.; Tsuruda, L. S.; Turecek, P. L.; Sims, J. PEGylated Biopharmaceuticals: Current Experience and Considerations for Nonclinical Development. *Toxicol. Pathol.* **2015**, *43*, 959−983.

(12) Swierczewska, M.; Lee, K. C.; Lee, S. What is the future of PEGylated therapies? *Expert Opin. Emerging Drugs* **2015**, *20*, 531−536.

(13) Lipsky, P. E.; Calabrese, L. H.; Kavanaugh, A.; Sundy, J. S.; Wright, D.; Wolfson, M.; Becker, M. A. Pegloticase immunogenicity: the relationship between efficacy and antibody development in patients treated for refractory chronic gout. *Arthritis Res. Ther.* **2014**, *16*, R60.

(14) Mima, Y.; Hashimoto, Y.; Shimizu, T.; Kiwada, H.; Ishida, T. Anti-PEG IgM Is a Major Contributor to the Accelerated Blood Clearance of Polyethylene Glycol-Conjugated Protein. *Mol. Pharmaceutics* **2015**, *12*, 2429−2435.

(15) Schellekens, H.; Hennink, W. E.; Brinks, V. The immunogenicity of polyethylene glycol: facts and fiction. *Pharm. Res.* **2013**, *30*, 1729−1734.

(16) Kaneda, Y.; Tsutsumi, Y.; Yoshioka, Y.; Kamada, H.; Yamamoto, Y.; Kodaira, H.; Tsunoda, S.-i.; Okamoto, T.; Mukai, Y.; Shibata, H.; et al. The use of PVP as a polymeric carrier to improve the plasma half-life of drugs. *Biomaterials* **2004**, *25*, 3259−3266.

(17) Kopeček, J.; Kopecková, P. HPMA copolymers: origins, early developments, present, and future. *Adv. Drug Delivery Rev.* **2010**, *62*, 122−149.

(18) Morgenstern, J.; Gil Alvaradejo, G.; Bluthardt, N.; Beloqui, A.; Delaittre, G.; Hubbuch, J. Impact of Polymer Bioconjugation on

Protein Stability and Activity Investigated with Discrete Conjugates: Alternatives to PEGylation. *Biomacromolecules* **2018**, *19*, 4250−4262.
(19) Mero, A.; Fang, Z.; Pasut, G.; Veronese, F. M.; Viegas, T. X. Selective conjugation of poly (2-ethyl 2-oxazoline) to granulocyte colony stimulating factor. *J. Controlled Release* **2012**, *159*, 353−361.
(20) Steinbach, T.; Becker, G.; Spiegel, A.; Figueiredo, T.; Russo, D.; Wurm, F. R. Reversible Bioconjugation: Biodegradable Poly-(phosphate)-Protein Conjugates. *Macromol. Biosci.* **2017**, *17*, No. 9.
(21) Pelosi, C.; Duce, C.; Wurm, F. R.; Tinè, M. R. Effect of Polymer Hydrophilicity and Molar Mass on the Properties of the Protein in Protein−Polymer Conjugates: The Case of PPEylated Myoglobin. *Biomacromolecules* **2021**, *22*, 1932−1943.
(22) Jain, S.; Hreczuk-Hirst, D. H.; McCormack, B.; Mital, M.; Epenetos, A.; Laing, P.; Gregoriadis, G. Polysialylated insulin: synthesis, characterization and biological activity in vivo. *Biochim. Biophys. Acta, Gen. Subj.* **2003**, *1622*, 42−49.
(23) Mansfield, K. M.; Maynard, H. D. Site-Specific Insulin-Trehalose Glycopolymer Conjugate by Grafting from Strategy Improves Bioactivity. *ACS Macro Lett.* **2018**, *7*, 324−329.
(24) Mondal, K.; Mehta, P.; Mehta, B. R.; Varandani, D.; Gupta, M. N. A bioconjugate of Pseudomonas cepacia lipase with alginate with enhanced catalytic efficiency. *Biochim. Biophys. Acta, Proteins Proteomics* **2006**, *1764*, 1080−1086.
(25) Mero, A.; Campisi, M. Hyaluronic acid bioconjugates for the delivery of bioactive molecules. *Polymers* **2014**, *6*, 346−369.
(26) Paleos, C. M.; Sideratou, Z.; Tsiourvas, D. Drug Delivery Systems Based on Hydroxyethyl Starch. *Bioconjugate Chem.* **2017**, *28*, 1611−1624.
(27) Belén, L. H.; Rangel-Yagui, C. dO.; Beltrán Lissabet, J. F.; Effer, B.; Lee-Estevez, M.; Pessoa, A.; Castillo, R. L.; Farías, J. G. From Synthesis to Characterization of Site-Selective PEGylated Proteins. *Front. Pharmacol.* **2019**, *10*, No. 1450.
(28) Francis, G.; Fisher, D.; Delgado, C.; Malik, F.; Gardiner, A.; Neale, D. PEGylation of cytokines and other therapeutic proteins and peptides: the importance of biological optimisation of coupling techniques. *Int. J. Hematol.* **1998**, *68*, 1−18.
(29) Wallat, J. D.; Rose, K. A.; Pokorski, J. K. Proteins as substrates for controlled radical polymerization. *Polym. Chem.* **2014**, *5*, 1545−1558.
(30) Theodorou, A.; Liarou, E.; Haddleton, D. M.; Stavrakaki, I. G.; Skordalidis, P.; Whitfield, R.; Anastasaki, A.; Velonia, K. Protein-polymer bioconjugates via a versatile oxygen tolerant photoinduced controlled radical polymerization approach. *Nat. Commun.* **2020**, *11*, No. 1486.
(31) Magnusson, J. P.; Bersani, S.; Salmaso, S.; Alexander, C.; Caliceti, P. In Situ Growth of Side-Chain PEG Polymers from Functionalized Human Growth Hormone—A New Technique for Preparation of Enhanced Protein−Polymer Conjugates. *Bioconjugate Chem.* **2010**, *21*, 671−678.
(32) Salmaso, S.; Caliceti, P. Peptide and Protein Bioconjugation: A Useful Tool to Improve the Biological Performance of Biotech Drugs. In *Peptide and Protein Delivery*, Elsevier, 2011; pp 247−290.
(33) Kovaliov, M.; Allegrezza, M. L.; Richter, B.; Konkolewicz, D.; Averick, S. Synthesis of lipase polymer hybrids with retained or enhanced activity using the grafting-from strategy. *Polymer* **2018**, *137*, 338−345.
(34) Pelegri-O'Day, E. M.; Maynard, H. D. Controlled radical polymerization as an enabling approach for the next generation of protein−polymer conjugates. *Acc. Chem. Res.* **2016**, *49*, 1777−1785.
(35) Averick, S.; Simakova, A.; Park, S.; Konkolewicz, D.; Magenau, A. J.; Mehl, R. A.; Matyjaszewski, K. ATRP under biologically relevant conditions: grafting from a protein. *ACS Macro Lett.* **2012**, *1*, 6−10.
(36) Sumerlin, B. S. Proteins as Initiators of Controlled Radical Polymerization: Grafting-from via ATRP and RAFT. *ACS Macro Lett.* **2012**, *1*, 141−145.
(37) Messina, M. S.; Messina, K. M. M.; Bhattacharya, A.; Montgomery, H. R.; Maynard, H. D. Preparation of biomolecule-polymer conjugates by grafting-from using ATRP, RAFT, or ROMP. *Prog. Polym. Sci.* **2020**, *100*, No. 101186.
(38) Liu, X.; Gao, W. Precision Conjugation: An Emerging Tool for Generating Protein−Polymer Conjugates. *Angew. Chem., Int. Ed.* **2021**, *60*, 11024−11035.
(39) Yaşayan, G.; Saeed, A. O.; Fernández-Trillo, F.; Allen, S.; Davies, M. C.; Jangher, A.; Paul, A.; Thurecht, K. J.; King, S. M.; Schweins, R.; et al. Responsive hybrid block co-polymer conjugates of proteins−controlled architecture to modulate substrate specificity and solution behaviour. *Polym. Chem.* **2011**, *2*, 1567−1578.
(40) Simakova, A.; Averick, S. E.; Konkolewicz, D.; Matyjaszewski, K. Aqueous ARGET ATRP. *Macromolecules* **2012**, *45*, 6371−6379.
(41) Wang, X.; Yadavalli, N. S.; Laradji, A. M.; Minko, S. Grafting through Method for Implanting of Lysozyme Enzyme in Molecular Brush for Improved Biocatalytic Activity and Thermal Stability. *Macromolecules* **2018**, *51*, 5039−5047.
(42) Kaupbayeva, B.; Murata, H.; Lucas, A.; Matyjaszewski, K.; Minden, J. S.; Russell, A. J. Molecular Sieving on the Surface of a Nano-Armored Protein. *Biomacromolecules* **2019**, *20*, 1235−1245.
(43) Munasinghe, A.; Mathavan, A.; Mathavan, A.; Lin, P.; Colina, C. M. Atomistic insight towards the impact of polymer architecture and grafting density on structure-dynamics of PEGylated bovine serum albumin and their applications. *J. Chem. Phys.* **2021**, *154*, No. 075101.
(44) Kaupbayeva, B.; Boye, S.; Munasinghe, A.; Murata, H.; Matyjaszewski, K.; Lederer, A.; Colina, C. M.; Russell, A. J. Molecular Dynamics-Guided Design of a Functional Protein−ATRP Conjugate That Eliminates Protein−Protein Interactions. *Bioconjugate Chem.* **2021**, *32*, 821−832.
(45) Robert-Nicoud, G.; Evans, R.; Vo, C.-D.; Cadman, C. J.; Tirelli, N. Synthesis, self-assembly and (absence of) protein interactions of poly(glycerol methacrylate)-silicone macro-amphiphiles. *Polym. Chem.* **2013**, *4*, 3458−3470.
(46) Haigh, R.; Rimmer, S.; Fullwood, N. J. Synthesis and properties of amphiphilic networks. 1: the effect of hydration and polymer composition on the adhesion of immunoglobulin-G to poly-(laurylmethacrylate-stat-glycerolmonomethacrylate-stat-ethylene-glycol-dimethacrylate) networks. *Biomaterials* **2000**, *21*, 735−739.
(47) Rimmer, S.; Johnson, C.; Zhao, B.; Collier, J.; Gilmore, L.; Sabnis, S.; Wyman, P.; Sammon, C.; Fullwood, N. J.; MacNeil, S. Epithelialization of hydrogels achieved by amine functionalization and co-culture with stromal cells. *Biomaterials* **2007**, *28*, 5319−5331.
(48) Patrucco, E.; Ouasti, S.; Vo, C. D.; De Leonardis, P.; Pollicino, A.; Armes, S. P.; Scandola, M.; Tirelli, N. Surface-Initiated ATRP Modification of Tissue Culture Substrates: Poly(glycerol monomethacrylate) as an Antifouling Surface. *Biomacromolecules* **2009**, *10*, 3130−3140.
(49) Mequanint, K.; Patel, A.; Bezuidenhout, D. Synthesis, Swelling Behavior, and Biocompatibility of Novel Physically Cross-Linked Polyurethane-block-Poly(glycerol methacrylate) Hydrogels. *Biomacromolecules* **2006**, *7*, 883−891.
(50) Ragupathy, L.; Millar, D. G.; Tirelli, N.; Cellesi, F. An Orthogonal Click-Chemistry Approach to Design Poly(glycerol monomethacrylate)-based Nanomaterials for Controlled Immunostimulation. *Macromol. Biosci.* **2014**, *14*, 1528−1538.
(51) De Leonardis, P.; Cellesi, F.; Tirelli, N. Tuning the properties of hybrid SiO2/ poly(glycerol monomethacrylate) nanoparticles for enzyme nanoencapsulation. *Colloids Surf., A* **2019**, *580*, No. 123734.
(52) Giacomelli, C.; Schmidt, V.; Borsali, R. Nanocontainers Formed by Self-Assembly of Poly(ethylene oxide)-b-poly(glycerol monomethacrylate)−Drug Conjugates. *Macromolecules* **2007**, *40*, 2148−2157.
(53) Moncalvo, F.; Lacroce, E.; Franzoni, G.; Altomare, A.; Fasoli, E.; Aldini, G.; Sacchetti, A.; Cellesi, F. Protein-friendly atom transfer radical polymerisation of glycerol(monomethacrylate) in buffer solution for the synthesis of a new class of polymer bioconjugates. *React. Funct. Polym.* **2022**, *175*, No. 105264.
(54) da Silva Freitas, D.; Abrahão-Neto, J. Batch purification of high-purity lysozyme from egg white and characterization of the enzyme modified by PEGylation. *Pharm. Biol.* **2010**, *48*, 554−562.

https://doi.org/10.1021/acs.macromol.2c00783
Macromolecules 2022, 55, 7454−7468

(55) Tao, L.; Mantovani, G.; Lecolley, F.; Haddleton, D. M. α-Aldehyde Terminally Functional Methacrylic Polymers from Living Radical Polymerization: Application in Protein Conjugation "Pegylation". *J. Am. Chem. Soc.* **2004**, *126*, 13220−13221.
(56) Krys, P.; Matyjaszewski, K. Kinetics of Atom Transfer Radical Polymerization. *Eur. Polym. J.* **2017**, *89*, 482−523.
(57) Pfister, D.; Morbidelli, M. Process for protein PEGylation. *J. Controlled Release* **2014**, *180*, 134−149.
(58) Dozier, J. K.; Distefano, M. D. Site-Specific PEGylation of Therapeutic Proteins. *Int. J. Mol. Sci.* **2015**, *16*, 25831−25864.
(59) Lee, H.; Jang, I. H.; Ryu, S. H.; Park, T. G. N-Terminal Site-Specific Mono-PEGylation of Epidermal Growth Factor. *Pharm. Res.* **2003**, *20*, 818−825.
(60) Gao, W.; Liu, W.; Mackay, J. A.; Zalutsky, M. R.; Toone, E. J.; Chilkoti, A. In situ growth of a stoichiometric PEG-like conjugate at a protein's N-terminus with significantly improved pharmacokinetics. *Proc. Natl. Acad. Sci. U.S.A.* **2009**, *106*, 15231−15236.
(61) Chen, D.; Disotuar, M. M.; Xiong, X.; Wang, Y.; Chou, D. H.-C. Selective N-terminal functionalization of native peptides and proteins. *Chem. Sci.* **2017**, *8*, 2717−2722.
(62) Böttger, R.; Hoffmann, R.; Knappe, D. Differential stability of therapeutic peptides with different proteolytic cleavage sites in blood, plasma and serum. *PLoS One* **2017**, *12*, No. e0178943.
(63) Abreu, C. M. R.; Fu, L.; Carmali, S.; Serra, A. C.; Matyjaszewski, K.; Coelho, J. F. J. Aqueous SARA ATRP using inorganic sulfites. *Polym. Chem.* **2017**, *8*, 375−387.
(64) Odom, O. W.; Kudlicki, W.; Kramer, G.; Hardesty, B. An Effect of Polyethylene Glycol 8000 on Protein Mobility in Sodium Dodecyl Sulfate−Polyacrylamide Gel Electrophoresis and a Method for Eliminating This Effect. *Anal. Biochem.* **1997**, *245*, 249−252.
(65) Pang, Y.; Liu, J.; Qi, Y.; Li, X.; Chilkoti, A. A Modular Method for the High-Yield Synthesis of Site-Specific Protein−Polymer Therapeutics. *Angew. Chem., Int. Ed.* **2016**, *55*, 10296−10300.
(66) Zheng, C. Y.; Ma, G.; Su, Z. Native PAGE eliminates the problem of PEG−SDS interaction in SDS-PAGE and provides an alternative to HPLC in characterization of protein PEGylation. *Electrophoresis* **2007**, *28*, 2801−2807.
(67) Lucius, M.; Falatach, R.; McGlone, C.; Makaroff, K.; Danielson, A.; Williams, C.; Nix, J. C.; Konkolewicz, D.; Page, R. C.; Berberich, J. A. Investigating the Impact of Polymer Functional Groups on the Stability and Activity of Lysozyme−Polymer Conjugates. *Biomacromolecules* **2016**, *17*, 1123−1134.
(68) Veronese, F. M.; Caliceti, P.; Schiavon, O. Branched and Linear Poly(Ethylene Glycol): Influence of the Polymer Structure on Enzymological, Pharmacokinetic, and Immunological Properties of Protein Conjugates. *J. Bioact. Compat. Polym.* **1997**, *12*, 196−207.
(69) Wurm, F.; Dingels, C.; Frey, H.; Klok, H. A. Squaric acid mediated synthesis and biological activity of a library of linear and hyperbranched poly(glycerol)-protein conjugates. *Biomacromolecules* **2012**, *13*, 1161−71.
(70) Schuster, J.; Koulov, A.; Mahler, H. C.; Detampel, P.; Huwyler, J.; Singh, S.; Mathaes, R. In Vivo Stability of Therapeutic Proteins. *Pharm. Res.* **2020**, *37*, No. 23.
(71) Werle, M.; Bernkop-Schnürch, A. Strategies to improve plasma half life time of peptide and protein drugs. *Amino Acids* **2006**, *30*, 351−367.
(72) Karstad, R.; Isaksen, G.; Wynendaele, E.; Guttormsen, Y.; De Spiegeleer, B.; Brandsdal, B. O.; Svendsen, J. S.; Svenson, J. Targeting the S1 and S3 subsite of trypsin with unnatural cationic amino acids generates antimicrobial peptides with potential for oral administration. *J. Med. Chem.* **2012**, *55*, 6294−6305.
(73) Knubovets, T.; Osterhout John, J.; Connolly Peter, J.; Klibanov Alexander, M. Structure, thermostability, and conformational flexibility of hen egg-white lysozyme dissolved in glycerol. *Proc. Natl. Acad. Sci. U.S.A.* **1999**, *96*, 1262−1267.
(74) Lutz, J.-F. Thermo-Switchable Materials Prepared Using the OEGMA-Platform. *Adv. Mater.* **2011**, *23*, 2237−2243.
(75) Lutz, J.-F. Polymerization of oligo(ethylene glycol) (meth)-acrylates: Toward new generations of smart biocompatible materials. *J. Polym. Sci., Part A: Polym. Chem.* **2008**, *46*, 3459−3470.
(76) Tao, Q.; Li, A.; Liu, X.; Ma, R.; An, Y.; Shi, L. Protecting enzymes against heat inactivation by temperature-sensitive polymer in confined space. *Phys. Chem. Chem. Phys.* **2011**, *13*, 16265−16271.

https://doi.org/10.1021/acs.macromol.2c00783
Macromolecules 2022, 55, 7454−7468